Development and testing of mechanically stable Vanadium redox flow battery

Bogdan Molchanov

If historians now see the turn of the 19th century as the dawn of the industrial revolution,
I hope they will see the turn of the 21s t century as the dawn of the energy revolution.

Rob Routs, Executive Director

Royal Dutch Shell plc, Apeldoorn, June 2007

Degree Thesis

Plastics Technology

2016

Dergree Thesis	
Arcada	
Degree Programme:	Plastics Technology
Identification number:	15435
Author:	Bogdan Molchanov
Title:	Development and testing of mechanically stable Vanadium redox flow battery
Supervisor (Arcada):	Stewart Makkonen-Craig
Commissioned by:	

Abstract:

This thesis work is concerned with electrochemical energy storage and conversion technology based on vanadium chemistry. This thesis is continuation of a work done at Arcada in summer 2015 and is expected to become a foundation for future research in the flow battery area. The major objective of this study was to build a prototype of vanadium flow battery that is robust enough to be analyzed and compared against flow batteries of other research groups. The work is broken down into four smaller parts. In the first part a literature review of flow batteries was compiled. The working principles and history of flow batteries and their electrolyte compositions were reviewed. In the second part, vanadium electrolyte production and monitoring methods were studied. The method of producing stock electrolyte from available reagents was established and UV-Vis spectra of the four pertinent oxidation states of vanadium were obtained. The spectra were found to match closely those reported by other research groups. The UV-Vis spectra were then correlated to electrolyte compositions and methods for electrolyte state of charge monitoring were developed. In the third part, improvements to the design and assembly of a battery test station and its components were conceived, evaluated and in some cases implemented. Modifications to the existing battery test station were favored over building a completely new test station. The modifications aimed primarily at eliminating notable electrolyte leakage in the reaction center and other critical spots. In the fourth part, experiments were performed to characterize the battery by undergoing charging and discharging cycles. Electrical data were analyzed to determine the power and efficiency of the battery. The peak power was found to be 0.15 W/cm^2, which is close to what other groups have reported. The efficiency of the battery was 60%, which is lower than the 90% efficiencies reported by other groups.

Keywords:	Vanadium, flow battery, energy storage and conversion, ion conducting membrane, efficiency
Number of pages:	69
Language:	English
Date of acceptance:	

List of Figures

List of Tables

List of abbreviations and acronyms

AQDS - 9,10-anthraquinone-2,7-disulphonic acid

CCV - Closed circuit voltage

DMFC - Direct methanol fuel cell

ETFE - Ethylene tetrafluoroethylene

GDL - Gas diffusion layer

IEA - International energy agency

PPEM - Proton exchange membrane

OCV - Open circuit voltage

PET - Polyethylene terephthalate

SoC - State of charge

VRFB or RFB - Vanadium redox flow battery

Contents

Acknowledgements

I would first like to thank my thesis supervisor Stewart Makkonen-Craig for constant support and advice during both my thesis and project work. He consistently allowed this paper to be my own work but would always be ready to guide me in the right direction whenever I ran into a trouble spot or had a question. I am also grateful to Björn Wiberg for technical advices and encouragement during my experimental work. His office door was always open for me whenever I needed advice.

Furthermore, I would like to express my gratitude to Mikael Paronen without whom this project would never be initiated. His trust in my problem solving skills had motivated me to delve into a completely new subject and as a result led me to writing of this paper. I would also like to thank “Arcadas Stipendiefonder” (SSF) committee for financial aid during the writing stage of my thesis. Without this support, I would not be able to reach logical culmination of my work within the deadlines.

Finally yet importantly, emotional support matters a lot at moments of high stress. I wish to thank my friends Anastasia Bozhko, Pavel Fahrutdinov and Inna Sharifgalieva for staying long hours with me in the laboratory, helping with experimental set ups and staying positive when everything else would go wrong.

1 Introduction

1.1 Background

In recent decades, the greenhouse effect along with depletion of fossil energy sources has drawn considerable attention towards the sustainability of energy production and consumption. Rising public awareness about environmental protection, lack of resources and stricter governmental policies have all inspired the development of next-generation clean energy technologies[1]. According to industrial energy producers, governments and research institutes such as the International Energy Agency (IEA), energy consumption worldwide along with CO_2 emissions will continue to increase for at least the near future[2] (see Figure 1).

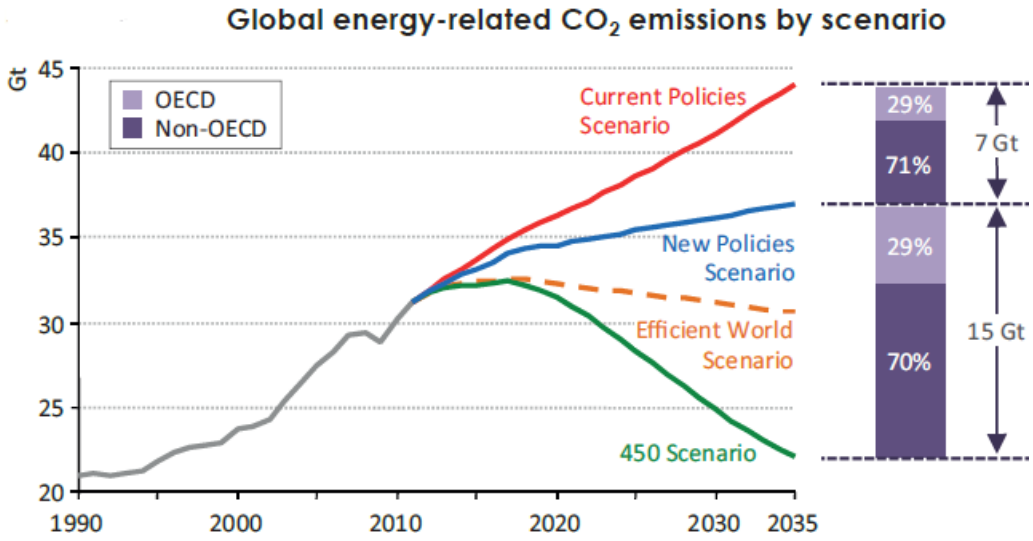

Figure 1. Scenarios showing Global CO_2 emissions by year 2035 as Projected by IEA[2]

By saving energy, switching to renewable technologies and improving efficiency of grids and power plants (Figure 2).

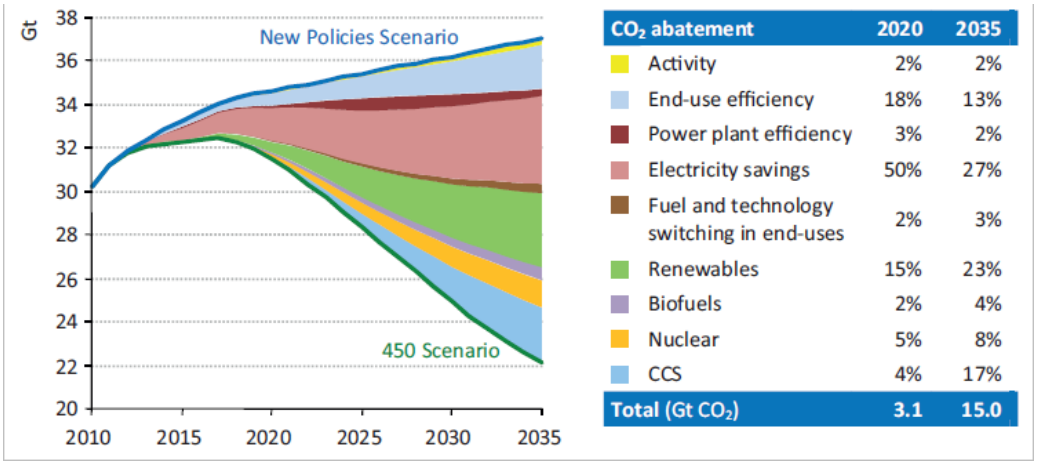

CO_2 abatement	2020	2035
Activity	2%	2%
End-use efficiency	18%	13%
Power plant efficiency	3%	2%
Electricity savings	50%	27%
Fuel and technology switching in end-uses	2%	3%
Renewables	15%	23%
Biofuels	2%	4%
Nuclear	5%	8%
CCS	4%	17%
Total (Gt CO_2)	3.1	15.0

Figure 2. Projections from the IAE showing (left) scenarios for global CO_2 emissions until year 2035, and (right) the impact of clean energy technologies on CO_2 emissions [2]

The message is clear in those projections. The CO_2 emission policies will tighten and there will be a trend towards both cleaner energy and smarter electricity usage in the coming decades (Figure 2).

Along with emerging and fast developing green technologies there will emerge new energy problems that require solution. For instance, wind and solar power are projected by Shell Company to produce over quarter of world's electricity by year 2050[3]. Wind and Sun are intermittent energy sources meaning there will be need to produce energy when winds do not blow and Sun does not shine and need to store surplus energy during the most productive periods. This problem brings people to the concepts of energy storage and conversion technologies. Below is a table of the popular energy storage technologies[4].

Table 1. Energy storage systems classified by energy conversion method.

Mechanical systems	*Electrical systems*	*Chemical systems*
Pumped hydro	Super Conducting Magnet	Li-ion battery
Compressed air storage	Super capacitors	Sodium - sulphur battery
Flywheel		Flow battery

One of the solutions to Energy storage system (ESS) requirements for renewable energies are flow batteries. Flow batteries are reduction-oxidation (redox) electrochemical cells, and they stand out from many other ESS systems (Figure 4) for a number of distinct advantages[5]:

- A flow battery has no limit to how much energy it can store. The amount of energy stored is dictated by the size of electrolyte storage tank, which can be a small bottle or a storage tank of size of a building.
- Power output can be increased or decreased independently of the energy capacity. This is possible because the reaction centre is located outside the electrolyte storage unlike in normal batteries. Hence increasing the area of reaction centre increases power output without affecting capacity.
- The environmental impact of a flow battery is very low due to well-known chemical compositions used and a long lifetime (over 20 years) of the system. The electrolyte's lifetime is practically limitless, requiring rebalancing.
- Response time (time during which battery gets activated and starts to produce energy) is a few milliseconds making it an ideal system for load levelling applications.
- The location where the flow battery can be installed has no specific requirements to landscape.

Due to possibility for customization, flow batteries could become economically more competitive and attract interest in different sectors and with varying energy and power demands.

The flow battery concept is multi-disciplinary and there are different chemical and technical solutions under development. Understanding flow battery technology and the impact of individual components on system efficiency is a challenging task that requires a lot of theoretical and practical preparation. This thesis is a continuation of a project work initially conducted at Arcada in summer 2015 and will focus mostly on vanadium flow battery technology of generation 1 (G1) type based on electrolytes comprising sulfuric acid and vanadium of concentrations up to 2 M.

1.2 Objectives

The main objective of this research project was to build a prototype vanadium-based flow battery system that could be used to characterize electrolytes, determine battery efficiency and understand how cell design can affect the battery's performance.

The initial attempts to build and characterize a vanadium-based battery were done during a summer project that was then continued by the experiments reported in this thesis. It quickly became evident that information on many vital aspects of vanadium battery preparation, such as electrolyte preparation and cell design, were not easily available from scientific publications. References from many selected articles, including older publications, led to a patented invention. For that reason, many of the methods reported here had to be re-established and verified for correctness. Establishing the electrolyte preparation method, the first prototype battery made on the basis of old fuel cell test station and attempts to determine battery's peak power and efficiencies had already been achieved in the summer. However, many obstacles remained in the progress towards a reliably functioning battery.

This thesis work is first in the field of flow batteries at Arcada, and it might be used as a foundation for further research in chemical energy storage and conversion technology. Therefore, an emphasis of this work was on reviewing current vanadium-based battery technologies, on developing electrolyte preparation methods, preparing battery operation guides, determining current battery performance parameters, and on further improvements to battery stability and state of charge monitoring methods.

The first major obstacle to safe operation of the battery was the notable leakage of electrolytes from the reaction centre. Not only is leakage a potential hazard for the user, but it also causes self-discharge of the battery. A review of battery designs and individual components was performed. Improvements to the existing system were evaluated against creating a completely new system from scratch.

The effort in summer 2016 focussed on investigating electrolyte preparation methods, but due to time limitations, little attention was devoted to monitoring methods for the state of charge of electrolytes during battery operation. Here, state of charge monitoring was achieved by UV-Vis spectrophotometry of the electrolytes. Due to a lack of relevant electronic equipment, the battery was not fully characterized in the summertime. In this work new options for recording the data from battery operation were screened and attempts to determine battery's efficiency and peak power were performed.

In summary, the objectives of this thesis work are:

- To build a reliable vanadium reduction-oxidation flow battery (VRFB)
- To investigate technical solutions to notable electrolyte leakage and cross-contamination problem in the first VRFB prototype
- To determine VRFB efficiencies and peak power
- To collect and analyse UV-Vis spectra of vanadium electrolytes for state of charge monitoring

2 Literature review

2.1 Introduction to Flow Battery Technology

2.1.1 Development and working principle of battery technology

A battery is generally a device that stores energy in the form of a chemical substance and delivers electric energy by consuming the chemicals[1]. Battery technology dates back a few hundreds of years but it is used in many applications in the modern world. The typical applications are portable electronics, electric vehicles, car engines, and power banks.

The battery technology started to develop after Alessandro Volta showed his first "voltaic pile" in 1798, which consisted of zinc-copper disks separated by wet paper. The zinc plate served as anode and copper as cathode, together creating redox pair, while wet paper was both separator and ion conductor. Electrochemistry is the subject that deals with such phenomena[1]. The idea of using chemically reactive substances to produce energy was quickly picked up by other scientists and it was soon evident that energy created from redox reactions can be extracted in the form of electricity by using a Voltaic cell or its equivalents. From there battery technology took off and many cell designs and redox pairs were found such as lead-acid, which is still used as car starter nowadays.

The Voltaic cell is different from normal chemical reactions by the fact that two substances do not react directly with each other. The reaction happens if[1]:

- There is potential difference between two separated substances (anode and cathode) immersed in solutions of respective substances.
- The substances can exist as aqueous solutions in the electrolyte (for reversible systems)
- There is a conducting wire connecting the two substances and thus creating electric circuit
- Ions in the electrolyte get replenished thus creating ionic circuit

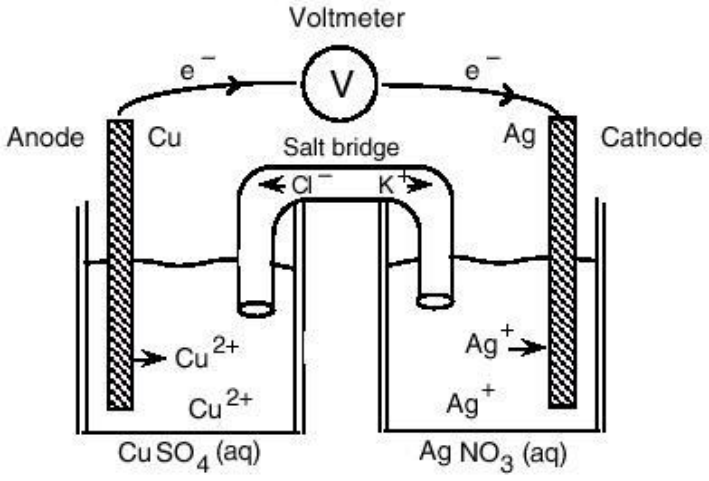

Figure 3. A schematic drawing of Cu-Ag Voltaic cell (Chang R., 2005, Chemistry, 8th Edition, Retrieved from: http://www.mhhe.com/

The substances are placed in two half-cells which, when connected by conducting wire and ion exchange system such as salt bridge or a membrane, generate electricity (see Figure 3).

The anode and cathode are chemically active substances on which the redox reaction occurs. Reduction reaction happens at the cathode, oxidation at the anode - simultaneously but in different half-cells. The wire acts as a medium through which electrons are transferred between the electrodes. The direction of electron flow is always from the anode to cathode when the battery is discharging. When the battery is charging, the electron flow is reversed. The salt bridge or ion-conducting membrane completes the circuit by allowing ions to transfer from one half-cell to another. Without rebalancing the electrolyte, the concentration of ions would reach a critical amount and the redox reaction would stop.

The electronegativity or potential difference between the two electrodes is measured in volts and the amount of charge transferred from anode to cathode per unit time is measured in amperes. A stack of cells can be connection in series and increasing the stack increases the total voltage. Batteries are said to be connected in parallel when cells are connected in such a way that cathodes and anodes are connected separately. In this case, the voltage stays constant but the current increases. By having a system of batteries connected both in series and in parallel, the required voltage and current can be achieved.

As battery technology developed, the versatility of configurations and redox pairs brought the need to compare between models in order to pick the best option for specific requirements. The four most important parameters for the battery to be considered are:

- Battery lifetime
- Specific energy density (W·h/kg) or Volumetric energy density (W·h/L)
- Specific power density (W/kg)
- Operation conditions

The battery lifetime is determined by amount of charges and discharges the battery can withstand before its performance becomes dissatisfactory[1]. During each charging and discharging cycle, redox components get involved in chemical reactions. Some of the reagents react with unwanted species such as contaminants, also the electrodes lose their initial structural properties overtime. Though marginal, the effect of unwanted side reactions builds up over time and impairs the cell's performance.

The specific energy density of the battery shows how much energy in watt-hours one kilogram of substance can produce, where one W·h is 3600 Joules. The amount of energy released per unit time depends on the potential difference of the electrodes, the mobility of ions and their weight. Therefore, small and mobile ions such as lithium are used in applications where high-energy content and low mass are required. The volumetric energy density is in most cases similar to specific density and differs by a con-

stant factor of substance density. In some cases, however the substance exists in many oxidation states and therefore has different densities.

The specific power density is the amount of power delivered per kilogram. Generally, peak power is considered in comparisons. Specific power is of special interest when there is limited space or weight for the application. (See Figure 4 for comparison of power densities for various technologies.)

Operation conditions are conditions at which a battery's performance is within acceptable limits. Often conditions refer to acceptable temperature and pressure windows. Li-ion, for instance, cannot be charged at temperatures below 0 °C while a sodium-sulphur battery requires at least 300 °C to operate.

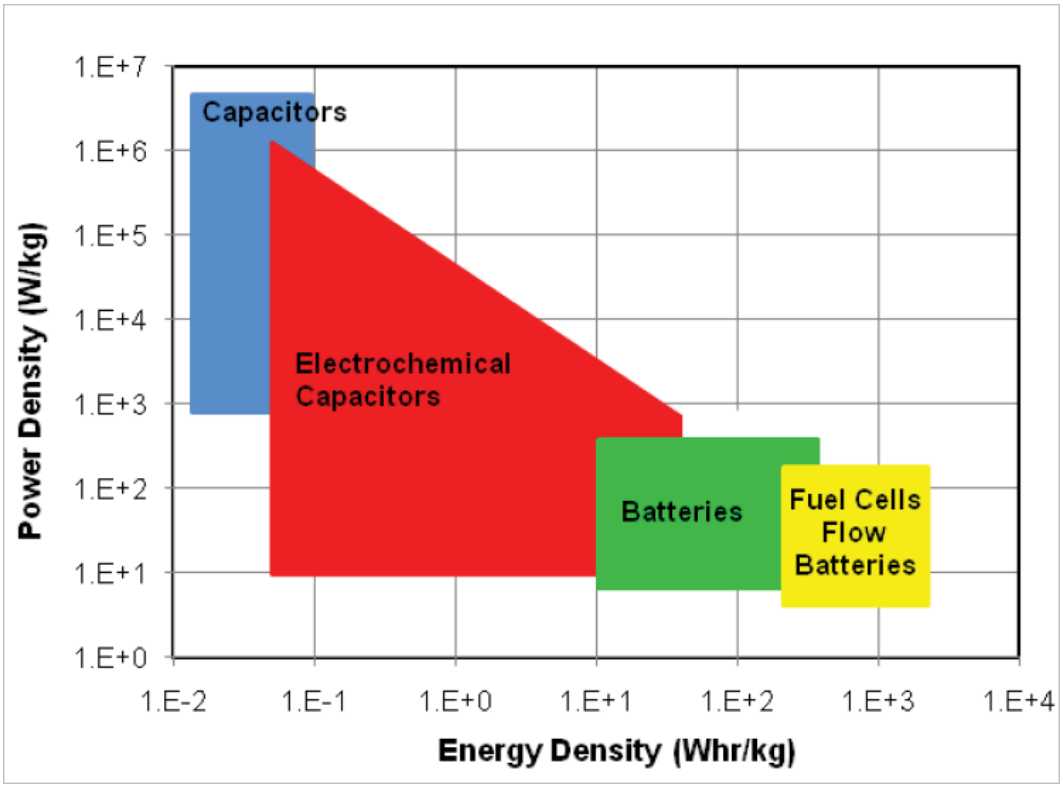

Figure 4. Power to energy density plots of energy storage systems (EES). (Trung Nguyen, 2010)

2.1.2 Flow Battery Technology

Batteries are a mature technology and they have found many applications in the past two centuries. Along with rising demands from the population, new challenges keep arousing still nowadays. Conventional batteries use the electrodes as sources of energy. The anode and cathode usually have different redox reaction rates and thus require that the surface areas of electrodes are different in order to meet the balance point. In addition, the electrodes are constantly subject to physical and chemical changes, so they wear out over time. Since electrodes contain reaction pairs, the battery becomes limited to its own volume. If one wants to increase energy capacity, the volume of the whole system has to be increased which also leads to an increase in power. Most batteries are intolerant to deep discharge cycles and, once out of order, need to be disposed[4]. Flow

battery technology has managed to overcome some of the limitations of conventional batteries: see Table 2 for a comparison of their technological parameters.

Table 2. A comparison between Galvanic and Flow battery technologies.

	Deep discharge	Lifetime	Environmental impact	Energy to Power ratio	Energy range	Electrode
Galvanic battery	Intolerant	~1000 cycles	High-medium	Hard to adjust	Few Wh-100kWh	Fuel + redox centre
Flow battery	Tolerant	>10000 cycles	Medium-low	Scalable	Few kWh - 100MWh	Only redox centre

A comparison of normal battery and flow battery diagrams is presented below (see Fig. 5a and 5b). In a conventional battery, and in an alkaline battery in particular, the reaction centre and energy storage are inside the case. The redox pair exists in the solid state and are part of the electrodes.

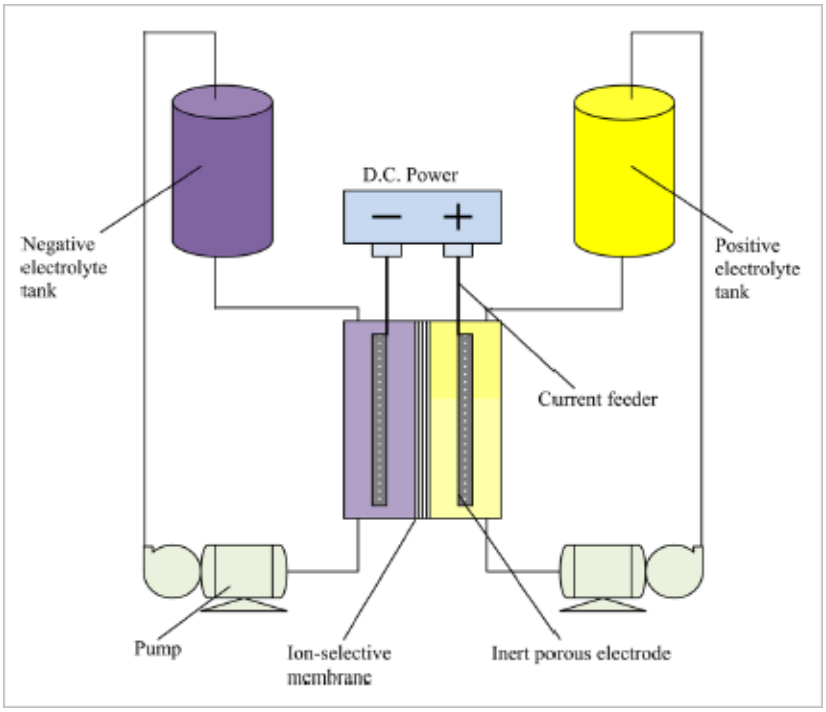

Figure 5b. A diagram of a flow battery. (Parasuraman, 2012)

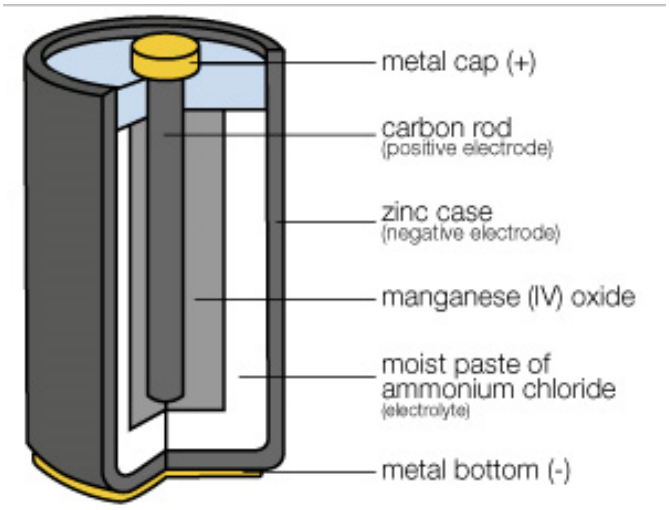

Figure 5a. A diagram of typical alkaline battery. Extracted from: http://techsavvymama.com/2014/02/, Access date: 22/11/2015

In the flow battery electrolyte, the reservoirs are kept outside the reaction centre. The redox pair is in a liquid state dissolved in the supporting electrolytes, which are circulated through the reaction centre using pumping units. The supporting electrolytes act as a solvent and in some cases as source of ions for maintaining reaction balance. The electrodes work as current collectors but do not take part in the redox reaction; they may work as catalysts in some cases.

The flow battery consists of four building blocks[6]:

- Two electrolyte storage tanks for holding charged and discharged electrolytes
- Reduction-oxidation centre - a cell or a stack of cells connected in parallel or/and in series
- Pumping units that enable circulation of electrolytes from reservoirs through the redox centre. The pump is the only mechanically moving part of the flow battery.
- Connection to grid (to load and source in the lab scale).

The electrolytes are pumped in a hydraulic circuit from reservoirs to the redox centre and back into the reservoirs until the battery is charged or discharged. During charging, external load is applied to the system and during discharging, energy is retrieved from spontaneous reaction.

The main part of the flow battery, reaction centre, comprises:

- Proton-exchange membrane (PEM)
- Electrode material (carbon paper, for instance)
- Conductive material with electrolyte flow channels (graphite, for instance)
- Sealing and leakage prevention material
- Current collectors (optional; graphite blocks conduct current well enough)

More detailed information on the chemistry and mechanical structure of an RFB will be given in sections 2.3 and 2.5.

2.1.3 Brief history of Flow Battery Development

The first working RFBs were developed by NASA in 1973 and patented by L.H. Thaller[5, 7]. A number of potential redox couples were investigated and the most promising couples were found to be iron-titanium (50% Coulombic efficiency) and iron-chromium (95% Coulombic efficiency). The Fe/Cr battery was developed and tested[7]. The battery employed Fe(II)/Fe(III) and Cr(II)/Cr(III) electrolytes, where (II) and (III) are the oxidation states, and their concentrations correspond to the state of charge of the battery. Soon it was evident that there are many challenges on the path of commercialization of RFB products. A few companies and research groups tried overcoming issues with flow batteries but did not achieve notable progress in the field. Some of the major challenges were[7]:

- Serious drop in energy efficiency during charge/discharge cycling
- Lack of good ion conducting membranes
- Cross-contamination of Fe and Cr species
- Expensive catalyst materials for Cr
- Low energy density

It was possible to increase energy density of the battery and develop better ion conducting membranes at the time but the problem of cross-contamination by metal ions could not be solved until 1984.

In 1984, Maria Skyllas-Kazacos and her research group proposed a battery designed to overcome above-mentioned problems[5, 8, 9]. The new electrolyte employed the unique properties of vanadium - a transition element that has four oxidation states. By proposing an all-vanadium (V^{2+}/V^{5+}) battery she eliminated the problem of efficiency drop, cross-contamination and use of expensive catalysts. The contamination of one half-cell by vanadium ions still occurred. It still would lead to charge loss but the lifetime and stability of the battery had increased and the system required little maintenance work. Vanadium flow batteries are currently the most promising metal-based energy storages and have recently started penetrating the markets[6].

Vanadium ions are used in both half-cells with the following half-cell reactions:

- Cathode reaction (positive half-cell)

$$\mathbf{VO^{2+} + H_2O \leftrightarrow VO_2^+ + 2H^+ + e^-} \qquad \textbf{Equation 2-1}$$

- Anode reaction (negative half-cell)

$$\mathbf{V^{3+} + e^- \leftrightarrow V^{2+}} \qquad \textbf{Equation 2-2}$$

- Full reaction:

$$\mathbf{VO_2^+ + V^{2+} + 2H^+ + e^- \leftrightarrow VO^{2+} + V^{3+} + H_2O} \qquad \textbf{Equation 2-3}$$

Where oxidation state of VO^{2+} is equivalent to V^{5+} and of VO_2^+ is equivalent to V^{4+}.

The four oxidation states and chemistry of vanadium were known prior to the invention. The real breakthrough was in new method of preparing the vanadium electrolytes. The solubility of V_2O_5 (vanadium pentoxide powder) in acid solutions is very low - approximately 0.1 M VO_2^+ per 2 M H_2SO_4[10]. The concentration of vanadium in the electrolyte, however, is directly related to energy and power density of the system[4]. M. Skyllas proposed a method of electrochemical oxidation of V^{4+} to V^{5+}, which allowed having concentrations of 2 M VO_2^+ in 2 M H_2SO_4 supporting electrolyte. The method consisted of dissolution of V^{4+} ions and then oxidation of them by means of electrical current and/or chemical reaction. Simultaneously, a method of dissolution of very cheap V_2O_5 ions into V^{5+} was developed by means of electrochemistry. While driving the concentrations up many times she also managed to significantly reduce the cost of raw materials for the electrolyte. The possibility of dissolving the vanadium salts by means of chemical and/or electrolytic reduction made the electrolyte cost affordable for commercial production[10].

The initial all-vanadium system was reported to have 73% round-trip efficiency but with a few enhancements in the cell structure, electrolyte composition and environment control, over 90% efficiency was achieved[5]. The round-trip efficiency means charging and discharging the battery fully to see how much energy it takes from the source compared to how much it gives back. The battery grabbed the attention of many companies and research groups and from there RFB development took off. Ion-exchange membranes were screened and selected for various redox pairs[5, 6]. The most promising membrane at the time for VRFB turned out to be Nafion - commercially available cation exchange membrane. Cheaper and/or more efficient membranes were later developed[11]. Some research groups concentrated on graphite channels and a vast number of mathematical models and experimental set ups were made for enhancing fluid dynamics inside the cell. Many electrodes were also screened for the RFB, and graphite/carbon electrodes were found to be cheap and corrosion resistant. Graphite also took part in vanadium redox reaction as a catalyst. The formation of -COOH groups on the electrode surface was reported to play the catalyst role and from there many methods of electrode surface functionalization were developed[5, 6, 12]. Nowadays many research groups concentrate on development of electrolytes with high energy densities and thermal stabilities[5, 6, 13].

Although the VRFB is the most promising metal-based battery it is important to mention that competing teams are trying to develop RFB based on organic materials. Even though the trend is quite new, a few successful projects were published and demonstrated to the public in recent years[14-16]. One promising battery was proposed by Michael Aziz and his team is an all-quinone battery[14]. The quinone is organic chemical that is a derivative of aromatic rings. The electrolyte is built of "9,10-anthraquinone-2,7-disulphonic acid" (AQDS) couple in diluted sulfuric acid. The AQDS has potential to overcome vanadium flow battery both in power density and production cost[14]. The AQDS has six points for attaching various end groups, which makes it possible to synthesize molecules for specific needs. For instance, if cross-contamination cannot be prevented by membrane, adding a long enough end-chain will make it physically impossible for quinone to migrate through the membrane. In case where all-organic system is needed, addition of hydroxyl end-groups might be able to create potential difference with normal AQDS.

2.2 Electrochemical principles of flow batteries

Electrochemistry is a very broad topic and is used or occurs naturally in many circumstances and in various environments. This section concentrates only on rechargeable battery related phenomena.

The rechargeable battery is essentially a chemical energy storage device that can both produce energy or receive it. The energy is released in the form of a current *I*, which has

units of *A* or coulombs/s. The electric charge *Q* (unit coulombs) is the fundamental unit of electricity[17]. 1 *A* is the amount of charge (*Q*) going through a cross-section of a wire per second.

$$Q = I \cdot t, \qquad 1Q = 6.241 \times 10^{18}\ electrons$$

The charge is created by accumulation of charged particles such as electrons or protons. By convention, electrons have negative and protons have positive charge. The ions may have both negative and positive charge. The current "*I*" flows only if there is a potential difference "*V*" between the terminals of the battery. The higher the voltage is between two points, the more energy electrons get in order to reach the opposite terminal. While the electrons flow, (create current) they can be used for producing work (*W*). The work can be done in terms of heat - by passing through a resistor (working principle of light bulbs), or in terms of movement - by creating electromagnetic field (working principle of motors). The simplest approximation of described electric circuit is Ohm's Law[1]:

$$\boldsymbol{V = IR} \qquad \textbf{Equation 2-4}$$

A VRFB has two electrodes at which the redox reactions take place and two electrolytes that carry the reacting substance and charge carriers (cations or anions). In order to make reactions happen a few points must be satisfied:

- There has to be potential difference between the opposing elements - the bigger the difference, the stronger the electromotive force becomes.
- All valence states of reagents in both electrolytes must be in a liquid state.
- The electrolyte has to be conductive (contains anions or cations such as protons).
- The electrodes are connected to a circuit to allow electrons to flow.

Vanadium reduction from V^{5+} to V^{2+} stages along with standard potentials (E^0) is shown in (Figure 6). The upper equation corresponds to catholyte (positive terminal) and the lowest equation corresponds to anolyte (negative terminal) - together they create a potential difference of 1.26 *V* for a fully charged battery (1.00 *V* - (-0.26 *V*) = 1.26 *V*). The middle equation describes a discharged cell. Even though there is potential difference, the potential difference is too low to deliver sufficient amount of energy.

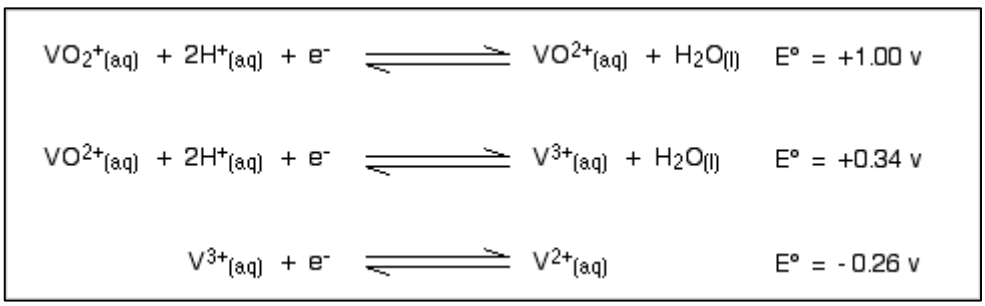

Figure 6. Redox reactions of vanadium with standard potentials for each reaction (Blanc. C, 2011)

The Nernst equation describes the open circuit voltage (OCV) between anolyte and catholyte taking into account ratios of concentrations of initial reagents to products[1]:

$$E = E^0 - \frac{RT}{nF}\ln[\frac{(c\mathrm{VO}_2^+) \times (c^2\mathrm{H}^+)}{c\mathrm{VO}^{2+}} \times \frac{c\mathrm{V}^{2+}}{c\mathrm{V}^{3+}}] \qquad \text{Equation 2-5}$$

Where E is the potential between terminals, R is the gas constant, T is temperature in Kelvin, F is Faraday's constant, n is amount of electrons altered at electrodes and c is concentration of respective substances in M. During the redox reaction the amount of reagents decreases while the amount of products increases. The reagents in this case are VO_2^+ and V^{2+}, the products are $\mathrm{VO}^{2+}$and V^{3+} in positive and negative half cells respectively. The simple model of redox reactions happening inside the cell can be seen from Figure 7.

The ratio of reagents to total concentration of species determines the state of charge (SoC) of the battery and can be derived from the Nernst equation and empirical data. SoC ranges between 100% and 0% and gives an estimate to how much more energy can be withdrawn from the system. The following equation can be used to express the SoC of a VRFB.

$$SoC = \left(\frac{c\mathrm{V}^{2+}}{c\mathrm{V}^{3+} + c\mathrm{V}^{2+}}\right) = \left(\frac{c\mathrm{VO}_2^+}{c\mathrm{VO}^{2+} + c\mathrm{VO}_2^+}\right) \qquad \text{Equation 2-6}$$

The cell Voltage and SoC will gradually decrease during operation until they reach zero meaning the product and reagent formation rates have reached equilibrium. Hence, the rate of creation of products is the same as the rate of creation of reagents.

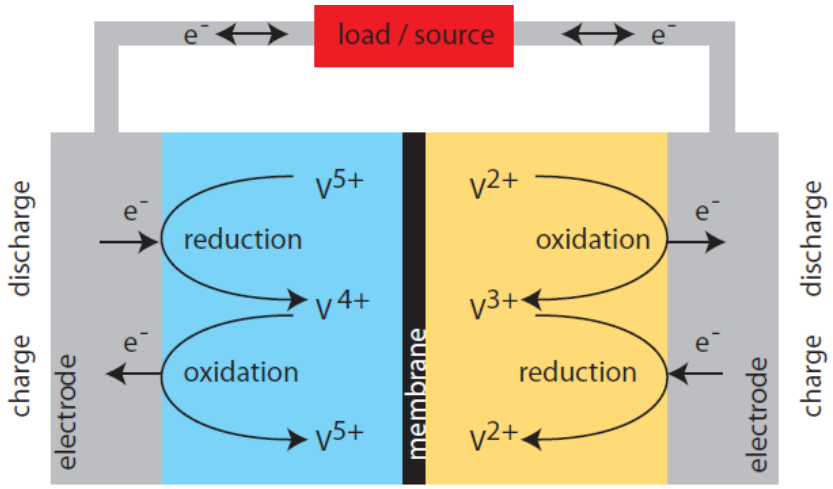

Figure 7. Simple model of redox reactions that happen inside the VRFB (Ya-Ching Tseng, 2011)

Knowing the numerical value of the equilibrium constant allows making assumptions on the extent of the reaction. In the case of the vanadium electrolyte in sulphuric acid,

the reaction favours product creation. As a result, voltage has to be applied to the system to supply enough energy in order to reverse the reaction and to recharge the battery.

In practice, the cell potential of a discharging battery or its closed circuit voltage (CCV) is less than 1.26 *V*. In contrast, when a battery is being charged, a voltage of higher than 1.26 *V* needs to be applied. Such deviation from theoretical value is caused by three resistance modes inside the cell: activation loss, ohmic loss and mass transport loss. When a cell is being discharged, some of the produced energy is consumed to overcome the resistances. When a battery is being charged, extra energy is required to overcome the resistances. For that reason, the resistances are also called overpotentials and below are given explanations to these mentioned overpotentials:

Activation overpotential is triggered at the initial stage of battery operation and determines the energy required to initiate redox reactions. It is due to the fact that a molecule has to overcome an energy barrier before it can get involved in a reaction. The factors that contribute to activation overpotential are temperature, distance of molecule from electrode surface, reaction rate constant and activation Gibb's energy. Activation overpotential is directly dependant on reaction rate of the elements. In the case of a flow cell, the half-cell with the slowest reaction rate species dictates how much voltage is consumed to trigger the reaction[4].

Concentration or mass transport overpotential is due to the difference between concentration of active species in bulk solution and in near proximity (a few nm) from an electrode surface (Figure 8). The vanadium species reach electrode surfaces via three possible mechanisms: diffusion (Brownian motion), migration due to electrostatic attraction between ions and electrodes and convection due to pressure, stirring or other mechanical means.

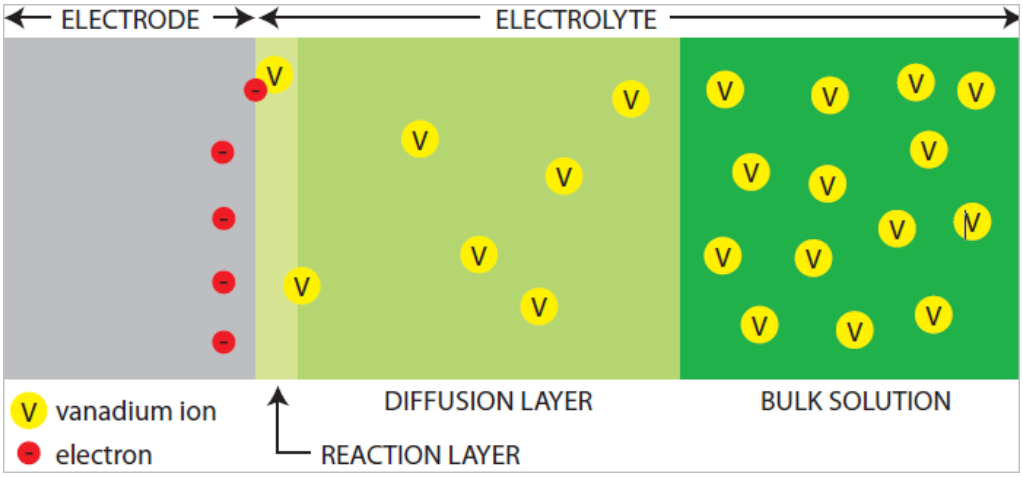

Figure 8. Reaction diagram for the half-cell. The reaction happens in a few nm width layer with certain speed dictated by reactivity of the substance. Diffusion to electrode needs to be faster than reaction rate in order to avoid triggering mass transport losses. (Blanc C., 2011)

Concentration overpotential is mostly a problem when a battery is almost fully discharged and the concentration of reactants is low - the diffusion through the gas diffusion layer (GDL) becomes slower than the reaction speed at the electrode surface. Concentration overpotential can also be triggered by reducing the electrolyte flow rate -

reaction at the electrode surface will become faster than diffusion from the bulk solution.

Ohmic/Ionic overpotentials form due to electrical resistance of the components in the circuit. Most of the losses come from imperfect contact between electrodes, current collectors, impurities in electrolyte and conductivity of membrane (Figure 9). The ionic overpotential is due to electrical resistance inside the solution.

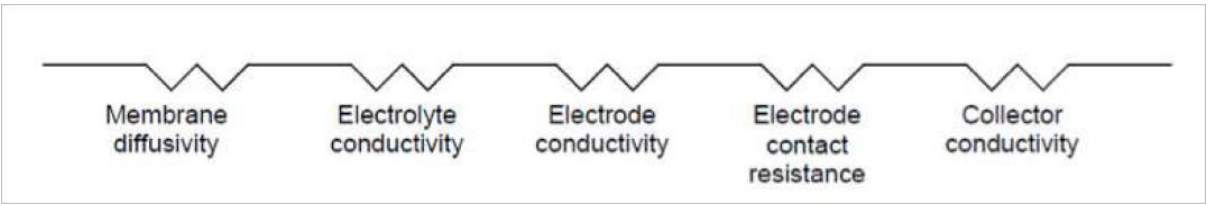

Figure 9. Factors contributing to increased ohmic/ionic loss. (Ya-Ching Tseng, 2011)[12]

Other overpotential contributing factors:

Due to an imbalance in reaction rates and reagent concentrations in the half-cell, during charging of the battery water might get electrolyzed instead of vanadium species, leading to evolution of hydrogen and voltage loss. The anolyte containing V^{2+} ions might get oxidized if the storage tank is not sealed properly, leading to imbalance in concentrations and voltage losses. The crossover of vanadium species through membrane inevitably leads to self-discharge of the battery and decreased voltage as a result. In addition, water molecules might migrate through the membrane, which also creates imbalance in reaction kinetics and concentrations.

Summing up all the loss factors during battery discharge cycle the graph in Figure 10 is obtained.

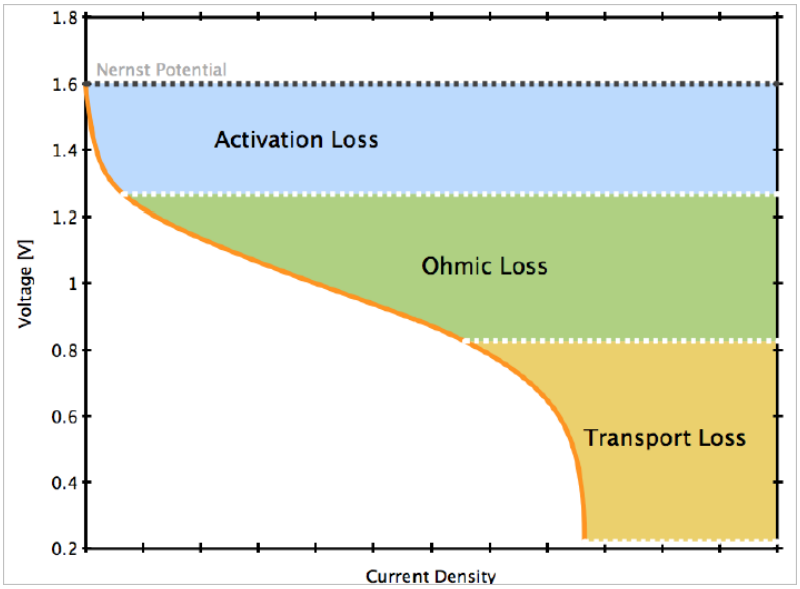

Figure 10. Activation overpotential is triggered at the beginning of operation to initiate the reaction; ohmic overpotential is constant and is due to contact resistances and impurities in the mechanical structure and electrolyte; concentration overpotential comes into force when concentration in bulk electrolyte becomes too low to supply enough ions to electrode per unit time (Zhijiang Tang, 2013)

The overpotentials contribute to energy losses inside the cell and the battery is generally built up from multiple cells, often referred to as a stack of cells. Figure 11 shows how

all of the above-mentioned factors affect performance of a flow cell. The voltage of a cell is therefore $U_{cell}(t) = U_{Nernst}(t) \pm U_{loss}(t)$. A plus sign is used when battery is being charged and minus sign is used when battery is being discharged. The equation determines input or output voltages respectively.

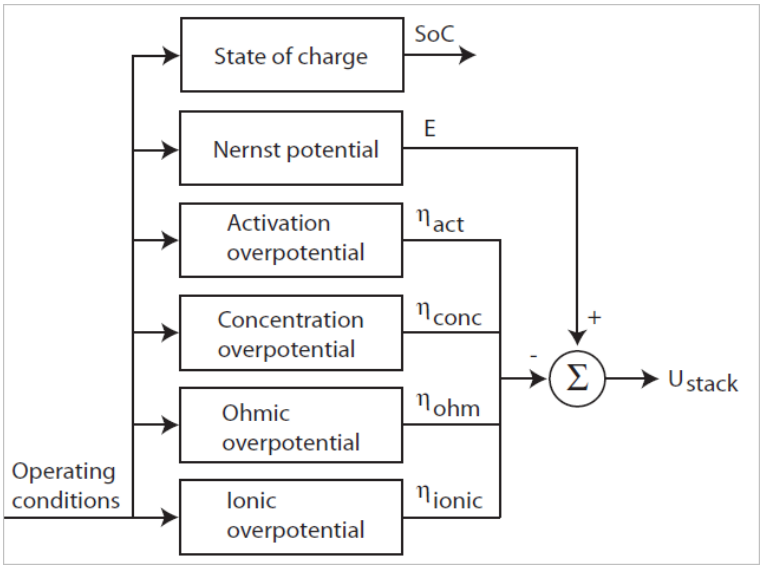

Figure 11. Factors, contributing to charging and discharging Voltage difference of the VRFB (Blanc C.,2011)

Determining parameters of the battery[4, 12]:

Due to the fact that there are many solutions to mechanical construction and chemical composition of batteries, a need arises to compare batteries between each other to find the best solution for the specific requirements of the application. It is usual that apart from battery cost considerations, outstanding performance is required in one of the below mentioned parameters.

Amount of charge stored in the battery - defines how many Coulombs (*C*) of charge are stored in the battery. It depends on the concentration of ions, volume of the storage tank and nature of electrochemical reaction:

$$Q = C(\text{vanadium}) \times V\text{tank} \times F \quad [C] \qquad \textbf{Equation 2-7}$$

Where Q is charge, C is concentration in M, V is volume and F is Faraday's constant (96 485 C/M).

Amount of energy stored - parameter defines the energy content of the system. It depends on the average cell voltage, amount of charge in the battery and amount of reactions happening simultaneously with same element. Since reactions happen in two half-cells, this parameter has to be divided by two:

$$E_{electrolyte} = 0.5 \times \frac{Ucell, avg \times Qcell}{3600} \quad [Wh] \qquad \textbf{Equation 2-8}$$

Energy density - a very important parameter allowing comparison of batteries of different compositions:

$$U_{electrolyte} = \frac{E_{electrolyte}}{V_{tank}} \quad \left[\frac{Wh}{L}\right] \qquad \text{Equation 2-9}$$

In theory 1.8 M VRFB cell corresponds to 35 Wh/L but due to internal losses, piping and side reactions the real energy density will correspond to only 20 Wh/L[4].

Energy efficiency - ratio of power produced during discharge to power consumed during recharging:

$$\mu_{energy} = \frac{\int P_{discharge} dt}{\int P_{charge}\, dt} \qquad \text{Equation 2-10}$$

Measuring energy efficiency is done by connecting the battery to a test station, and recording both voltage and current during charge-discharge cycle. The quotient of current-voltage products gives the experimental energy efficiency.

Coulombic efficiency - ratio of charge consumed to charge produced. It is always larger than energy efficiency:

$$\mu_{coulumbic} = \frac{\int I_{discharge} dt}{\int I_{charge}\, dt} = \frac{Q_{discharge}}{Q_{charge}} \qquad \text{Equation 2-11}$$

Coulombic efficiency is determined by keeping voltage constant during charge-discharge cycles and taking current readings. The ratio of the charge and discharge readings is the experimental Coulombic efficiency.

Voltage efficiency - is a measure of overpotential losses during operation at constant current:

$$\mu_{voltage} = \frac{\int U_{discharge} dt}{\int U_{charge}\, dt} \qquad \text{Equation 2-12}$$

Voltage efficiency is determined by keeping the current constant during charge – discharge cycles. Due to the above-mentioned overpotential losses (Figures 10 and 11), the voltage is different during charging and discharging of the battery. The ratio of the two readings gives voltage efficiency.

Since the energy of the battery (*E*) is calculated as a product of current and voltage over charging-discharging time:

$$\mu_{energy} = \mu_{coulumbic} \times \mu_{voltage} \qquad \text{Equation 2-13}$$

Equation 2-13 explains why μ_{energy} is smaller or in extreme cases equal to the other two efficiencies. Generally, $\mu_{energy} = 0.85$ is acceptable for energy storage system[14].

A battery's maximum power output can be found by gradually decreasing voltage and taking current readouts. Plotting power (*W*) versus voltage (*V*) or time (*t*) should give a parabolic graph and the peak power ($P = I \cdot V$) will be the maximum power output of the battery at the given SoC.

2.3 Mechanical Structure of VRFB

The flow battery is a complicated interdisciplinary apparatus that requires a lot of cell and material design. The whole system, however, can be broken down into single units that can be considered independently of each other. In Figure 5b, a schematic drawing on RFB illustrates that the battery has four main components some of which in turn are built of subcomponents. These subcomponents and other related components will now be described here in detail. All of the below mentioned components are generally used in VRFB.

- *Two electrolyte reservoirs*

The reservoirs are used as storage tanks for anolyte (V^{2+}, $V3^{+}$) and catholyte (V^{5+}, $V4^{+}$). The storage tanks can be of any volume - from a few mL to thousands of litres depending on the application it is used for. The bigger the volume of reservoirs, the more energy is stored in the battery. In the laboratory scale, volumes usually range between 20 and 1000 mL. Due to the fact that the vanadium electrolyte is usually dissolved in very acidic solutions such as sulphuric and/or hydrochloric acid, the material of storage tanks needs to be chemically inert. Usually, glass or plastic bottles are used for their transparency and corrosion resistance. The electrolyte tank needs to be well sealed to avoid evaporation, chemical spills or leakages. The anolyte containing reservoir requires an airtight design as both V^{2+} and V^{3+} ions get oxidised in the presence of oxygen gas leading to an imbalance in the system and energy losses[18]. The catholyte is less subject to redox reactions in the presence of air. On the other hand, V^{5+} ions that are found in the catholyte start to precipitate from solution at temperatures below 15 ℃ and above 40 ℃ [8]. Therefore, the catholyte has to be stored in a room with a controlled environment. There are many available storage tank designs and the simplest of them is two glass bottles with airtight screw caps. The screw caps have inlets and outlets with flexible and chemically inert pipes going through. The outlet pipe reaches the bottom of storage tank and takes fresh electrolyte for to the reaction centre while inlet pipe barely touches the surface of the electrolyte and brings used electrolyte back into system. Taking electrolytes from different height levels ensures that every portion of electrolyte between those two levels is being consumed. Some other designs rely on constant stirring, random mixing or integrated pump designs.

- *Two pumping units*

The pumping units are used to circulate fresh and used electrolytes between the reaction centre and the storage tanks. The pumps are actually the only moving parts of the system - easily replaceable and well-studied to date, making the whole system simple to operate and service, and to have a long lifetime. There are many designs of pumps that could be used in the system. Among the available designs, for laboratory scale a peristaltic pump is the perfect candidate. A peristaltic pump has a rotor with two or more rollers that come in contact with flexible tube containing electrolyte. The rollers push on the tube from outside, deform it and make liquid inside the tube follow the roller's motion, thus creating circulation without coming into contact with the electrolyte (Figure 12). The fact that electrolyte does not come in touch with rotor is of high importance

especially for the V^{2+} containing anolyte, which is subject to oxidation in presence of air or other contaminants. Generally, the pumping speeds of both electrolytes are the same. The flow rate needs to be altered in such a way as to not to trigger activation or mass transport overpotentials. In each design the flow speed requirement is unique and needs to be found experimentally.

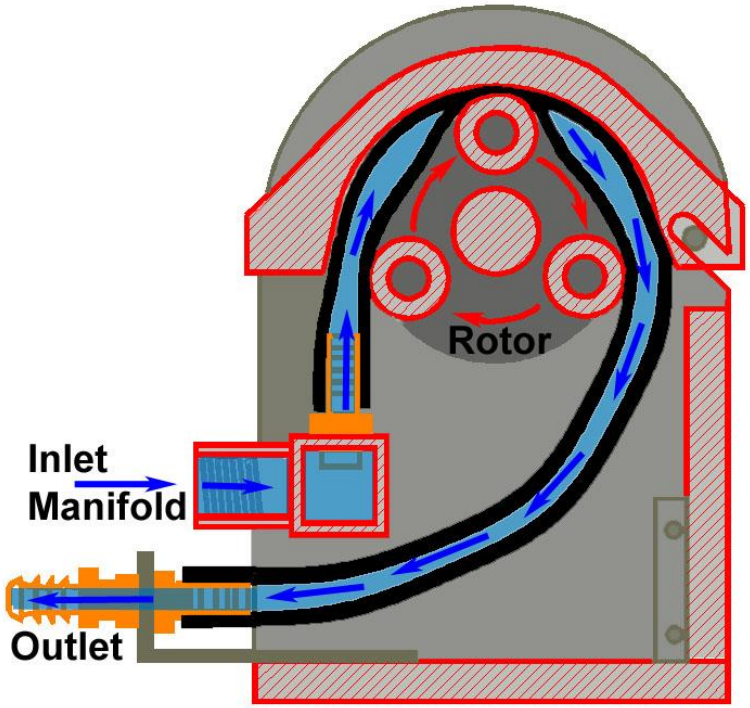

Figure 12. Schematic drawing of a peristaltic pump. (Ledebuhr Industries, Inc. Accessed from: http://www.proptec.com/pumps/technology.php Access date: 30/13/2015)

- *Load, power source and test station*

The load is any electrical device that draws energy from the battery. The power source is external source of energy that is being transferred to the battery. In general, the load and power source should have controllable voltages and/or current supplies or uptakes. Usually, a battery test station is also connected to a combined load and power source in order to record data from current and voltage measurements during charge and discharge cycles. The data can then be used to determine battery's coulombic, voltage and energy efficiencies, its stability, lifetime and peak power for the given cell. For a one-cell vanadium RFB the load/source should be able to supply between 1.5 and 2 *V* and consume between 0 and 1.2 *V*.

- *The cell or the cell stack*

The cell or a stack of cells is the heart and the reaction centre of the RFB. All reactions and chemical and electrochemical processes take place there. The electrolytes pumped from reservoirs simultaneously enter the cell, and the power supply or load is attached to the cell via cables to close the electrical circuit. The electrolytes do not mix inside the cell as they are separated by ion-exchange membrane that in theory only allows protons to transfer between the half-cells. The cell is built from four main subcomponents: see the schematic of the reaction centre below (Figure 13). On each side of the reaction cen-

tre electrolyte is pumped from its reservoir into an end plate. In the endplate, the electrolyte follows the flow channels between the inlet and outlet. The GDL is placed right on top of the flow channel area. Some of the electrolyte diffuses into the GDL or comes close enough so that redox reaction happens - the products return back into reservoirs via pipes. The protons freed during reaction go across the PEM to complete the ionic circuit while electrons are collected from the jack milled into the endplates.

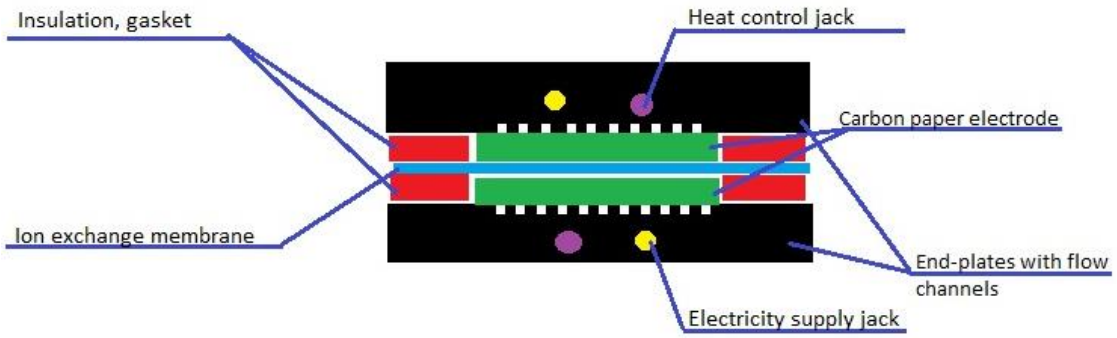

Figure 13. Schematic drawing of RFB reaction centre and its main componentsused in this study.

- *Graphite block with flow channels*

The graphite block in a VRFB is a multipurpose component that works as electrolyte distributor, support for the PEM and electrodes, conducts current and also works as a mechanical support for the reaction centre[4]. The main function of the block is the control of electrolyte flow. Even and controlled flow is achieved by milling flow channels into the graphite block - liquid follows the grooves in the space between inlet and outlet. There are many effective designs of flow channels, one of the most commonly used is the serpentine flow channel. Figure 14 illustrates various designs of flow channels. A serpentine flow channel does not allow liquid stagnation in dead ends, has only one direction to follow meaning electrolyte moves with the same speed at every point inside the cell and the path is of satisfactory length which gives enough time for redox reactions to happen. The interdigitated flow channel incorporates baffles that force electrolyte to diffuse into GDL in order to reach outlet. The interdigitated design is often used for gaseous electrolytes.

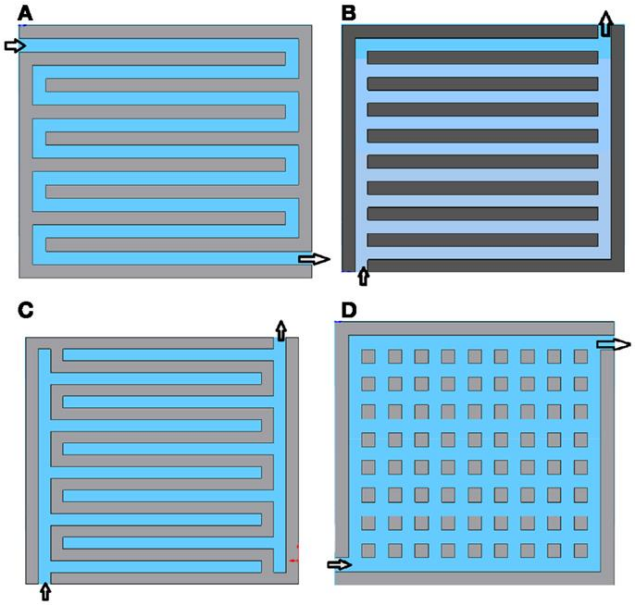

Figure 14. Flow channel designs. A - Serpentine; B - Parallel; C - Interdigitated, D - Pin. (Hong Liu, 2014). Retrieved from: http://www.frontiersin.org/Journal. Access date: 01/01/15

Along with being a guide for electrolyte flow, the plates have to also be electrically conductive and chemically inert. From the early stages of VRFB research, carbon/graphite was found to satisfy all these requirements at relatively low cost and fast availability. The fact that graphite is electrically conductive allows us to avoid using current collector plates in many designs - the current is collected directly from the plate through milled jack inserts. Due to the requirement of thermal stability, another jack is used for heat measurements inside the cell. It is unlikely, however, that the temperature inside the cell will exceed the critical maximum.

There are two endplates in one cell for the anolyte and catholyte, respectively. In the case of a stack of cells, endplates are only used at the very ends of stack and all the inside plates are bipolar and serve for both electrolytes at the same time. The bipolar plates are generally more complicated in design since they have to be electrically conductive but not permeable for liquids. Existing designs include plastic materials reinforced with metal and/or carbon particles for electrical conductivity in the desired direction. Older designs used two endplates instead of one bipolar plate, which greatly contributed to internal resistance, system weight and price increase.

- *Proton exchange membrane (PEM)*

The PEM is the key component of RFB. The membrane functions as a selective filter - it allows for transfer of cations such as protons in the case of a VRFB to keep the charge balanced in half-cells but prevents unwanted elements in the first compartment from penetrating to the other side of the membrane and eventually reacting and/or mixing with elements in the second compartment or vice versa. In the most simplified model, the PEM can be regarded as a porous film with pores of few nm diameter. The pores serve as channels for ion exchange. In order to make the pores selective to protons only, they are functionalized chemically with, typically, sulphuric acid for a while and stored in distilled water until use. In this manner, the pores or channels obtain functional

groups along the ion exchange path. Those charge-carrying end-groups allow cations to transfer through the membrane while acting as a repulsive barrier for anions. In reality, the repulsion can be overcome by electro-osmosis and unwanted species such as vanadium ions and water molecules will penetrate to the other side reducing the efficiency of the battery and its lifetime.

In the case of vanadium electrolytes, the vanadium ions of various charges react with each other and reduce the efficiency of the battery in the short term. In the long term, it is not a problem as no precipitation or degradation of the battery happens. The concentration misbalance can be altered by changing the polarity of the battery or by mixing both electrolytes and splitting into equal volumes occasionally. The commercially available Nafion® membranes, although very well studied, have many disadvantages for the RFB application. Among the problems is unwanted water and vanadium ion migration through the membrane leading to imbalance in concentrations and swelling of the membrane due to moisture uptake[12, 19]. Some research groups proposed modifications to the membrane and/or new membranes that better suit the needs of RFB. For instance, copolymerisation was used to increase the thickness of Nafion membranes and as a result decrease vanadium crossover. A porous sponge-like ion-conductive membrane was developed that showed higher stability and efficiency than Nafion. The sponge-like membrane was created by adding a positively charged crosslinked network around Nafion membrane. The crosslinked network greatly increases membrane stability and gives contribution to ion selectivity properties of Nafion[11]. The general requirements for a VRFB membrane are ion selectivity and conductivity, high chemical resistance, long service life and negligible water and vanadium crossover.

- *Gas diffusion layer (GDL)*

The GDL is inappropriate name in the case of RFBs. In flow batteries, the GDL serves as liquid diffusion layer and also as the electrode at which the reaction happens. The electrode has to be chemically resistive, electrically conductive, porous to facilitate ion transfer to membrane and possess a large surface area in order to support redox reactions. In the VRFB, the electrode material does not take part in redox reactions directly, therefore, it does not degrade and has a long lifetime. The best and cheapest material for such applications was found to be carbon felt or paper[5, 6]. In recent years carbon felt was used less and less while carbon paper technology from PEMFC (proton exchange membrane fuel cells) was reported to perform better and have longer lifetimes[19]. Carbon paper electrodes are commercially available products, which also makes them easy to purchase. After the electrolyte enters the flow channel it penetrates the porous electrode due to osmosis and pressure differences, and on the surface of electrode, a complicated redox reaction happens. Recent studies show that functional end-groups such as -CO and -NH_4 act as reaction catalysts[12, 19]. There are quite many ways to functionalize the surface of the electrode at the laboratory scale, e.g. heating in a NH_3 environment, plasma treatment and chemical doping.

- *Miscellaneous components*

In order to make a flow battery function, some supporting components are required. The electrode has to be in very close contact with the graphite plate and membrane so that contact resistance is minimized and useful area is increased. Therefore, mechanical pressure is used to clamp the whole cell together mechanically. There are various designs for clamping units. In some designs rigid plastic endplates with nuts and screws are used to clamp the system. Some other designs rely on hydraulic or pneumatic presses that make systems less mobile but more secure.

The reaction centre, pump and reservoirs are connected by an airtight tubing. The circuit is comprised of flexible, chemically resistant tubes, manifolds and tube connectors. Typical material choices are PTFE (Teflon ®) or PP (polypropylene) for availability, flexibility and relatively low cost. Manifolds and connectors are also made of plastic materials. Metal parts should be avoided from being used. Some deigns do not insulate the anolyte reservoir too well from coming into contact with oxygen. In such cases, additional purging system may be connected to the anolyte storage tank. The purging system could be nitrogen or carbon dioxide pressurized gas. When opened, the pressure from gas bottle pushes all air out, leaving the electrolyte in neutral atmosphere. In case of poor sealing design, purging has to be done during battery operation.

Sealing or gasket material is also used inside the cell as it can be seen from Figure 13. There the insulator has a number of functions. Firstly, it prevents graphite plates from coming in direct contact with each other, which would result in energy losses. Secondly, a gasket prevents electrolyte from leaking away from cell. The pressure build-up inside a cell can be huge, leading to electrolyte being forced outside its flow path and flowing outside the system. Last purpose of the gasket is to stop carbon paper or felt electrode from being crushed. Due to mechanical pressure from clamping unit, the paper is being compressed. At high pressure electrode might be compressed so much that its structure is no longer porous leading to poor electrolyte penetration and loss of active surface area. Sealing material serves as a barrier that does not allow electrode to be compressed beyond certain degree of porosity. Porosity is measured as a percentage of voids relative to materials volume. For instance, 90% porosity means that 10% of material's volume is occupied by actual material. Due to compression, volume decreases while amount of material stays constant - this leads to decrease in volume fraction of the pores. Typically, ETFE polymer is used as gasketing material for its chemical resistivity, gap-filling properties and high elastic modulus[19]. The gaskets are normally placed into grooves milled on the endplate surface but in some situations, they are just laid on by hand.

2.4 Capital cost of VRFB

Very important aspect of technology, although often ignored by engineers, is competition in the market. The factors that affect the costumer's choice are novelty, policies, cost and simplicity. Each factor has deep connections with social sciences and, therefore, could be discussed as a new topic. The VRFB technology is relatively new technology, picking up its popularity together with development of alternative energy technologies and energy saving policies. As the technology matured, it has reached a point where VRFB is almost maintenance-free, easy and safe to operate. That said VRFB has

full potential to enter the market and compete against other battery technologies. The financial competition, however, has greatest contribution of all. Rarely a costumer will pay more for a technology that has cheaper alternative. For that purpose, in this chapter a 6.4 kWh VRFB construction will be compared against Li-Ion based 6.4 kWh Tesla Powerwall (Table 3)[20]. The Tesla Powerwall was chosen for comparison as it has recently become a popular energy storage system in the households. For reader's interest, 6.4 kWh energy storage is equivalent to heat energy of 105 L of water stored at 50 ℃ above room temperature.

Table 3. Specifications for commercially available 6.4 kWh Tesla Powerwall[20].

Capacity	6.4 kWh	Depth of discharge	100%
Cost	2700 Euro	Efficiency	92%
Lifetime	10 years	Temperature	-20 to 50℃
Power	3.3 kW	Weight	100 kg

Using the Tesla Powerwall as a reference, a hypothetical model of 6.4 kWh VRFB with 3.3 kW output can be built. For 6.4 kWh system, using Equation 2-7 and Equation 2-8, the volume of electrolyte for VRFB becomes 221.1 L. The 221.1 L contains $221.1\ \mathrm{L} * 1.8\ \mathrm{M} = 400\ \mathrm{mol}$ of vanadium ions. If the raw material for electrolyte preparation was purchased in form of V_2O_5, molar weight of which is 182 g/mol, then $\frac{400}{2} M * 182\ \frac{g}{mol} = 37.5\ kg$ of powder is required. Additionally, around 40 L of concentrated Sulfuric acid would be required to produce solvent. For the power output of 3.3 kW, the reported value of power density for VRFB is $0.1\ \frac{W}{cm^2}\ or\ 1\ \frac{kW}{m^2}$. To reach 3.3 kW output, 3.3 m^2 of graphite plates is required. That also brings in need for around 6.6 and 3.3 m^2 of GDL and PEM, respectively.

The pricelist for critical components of VRFB is summarized in Table 4.

Table 4. Rough cost estimation of VRFB components.

Component	Unit price	Total price
Membrane[21]	~400 Eur/m^2	1320 Eur
GDL[22]	~100 Eur/m^2	660 Eur
V_2O_5[23]	~10 Eur/kg	375 Eur
Sulfuric acid[24]	~15 Eur/ L	600 Eur
Bipolar plate[25]	~480 Eur/m^2	800
Total	-	3755 Eur

The additional price of pumping units, connection to grid, storage tanks and tubes would be around 1300 Euros, making full system cost approximately 5000 Euros. The specifications of 6.4 kWh VRFB are presented in Table 5.

Table 5. Specifications of 6.4 *kWh* VRFB system.

Capacity	6.4 *kWh*	Depth of discharge	100%
Cost	5000 Euro	Efficiency	80%
Lifetime	~20 years	Temperature	-10 to 50℃
Power	3.3 *kW*	Volume	0.5 m^3

It is evident that for the same specifications, the Tesla Powerwall beats VRFB in price. However, because pumping units, connection to the grid and similar structural compo-

nents' cost does not change as the system is scaled up, the VRFB becomes more competitive. The GDL price here is taken from laboratory scale retailer, so the price could be much lower in reality. The membrane constitutes major part of VRFB cost and replacement of it with cheaper alternatives could easily decrease costs of VRFB. The bottom-line is, with currently commercially available materials the VRFB is not competitive in small-scale applications. On the other hand, there is ample space for improvements, so it can easily become a cheaper alternative to Powerwall in near future.

2.5 Chemical Structure of VRFB

The all-vanadium electrolyte is based on four possible oxidation states of vanadium: V^{2+}, V^{3+}, V^{4+} and V^{5+} corresponding to purple, green, blue and yellow colours respectively (see Figure 15). Vanadium was named after Vanadis - Scandinavian goddess of beauty exactly for the property of attaining large spectrum of colors in different chemical compositions and at various oxidation states. Vanadium is element 23 in periodic table with symbol V and atomic weight of 50.94 g/mol. It is a transition metal of silvery color, quite common in nature but only in chemically combined states.

Figure 15. Visual appearance of diluted vanadium electrolyte at corresponding charge. (Ya-Ching Tseng, 2011)

As it can be seen from Figure 8, VRFB is based on four oxidation states that are employed in two simultaneous electrode reactions :

$$V^{2+} \leftrightarrow V^{3+} + e^{-} \qquad \textbf{Equation 2-14}$$

$$V^{5+} + e^{-} \leftrightarrow V^{4+} \qquad \textbf{Equation 2-14}$$

Where discharging reaction reads from left to right and charging reads from right to left. The above equations are usually used for explaining simple model of how the battery works. In reality, the V^{5+} and V^{4+} ions contained in catholyte exist only in form of VO_2^+ and VO^{2+} oxides respectively. In order to keep the redox reaction balanced, water molecule needs to get involved in the reaction at positive electrode (Equation 2.2):

$$VO_2^+ + 2H^+ + e^{-} \leftrightarrow VO^{2+} + H_2O \qquad \textbf{Equation 2-2}$$

The anolyte contains vanadium ions in free form; therefore, first (Equation 2.1) remains unchanged. The full equation for simultaneous reaction then becomes (Equation 2.3):

$$VO_2^+ + V^{2+} + 2H^+ + e^{-} \leftrightarrow VO^{2+} + V^{3+} + H_2O \qquad \textbf{Equation 2-3}$$

Although there are many chemical compositions developed for VRFB the main components are:

- Vanadium ions and oxides that extract or store energy
- Supporting electrolyte that allows vanadium to stay in liquid form at all oxidation states and provides protons and anions that do not take direct part in redox reaction.
- Water that provides a source of protons for anode reaction.

In this work only vanadium batteries based on Sulfuric acid supporting electrolytes are studied. It is important to mention, however, that some research groups have achieved notable progress using other supporting electrolyte compositions, especially hydrochloric acid[6]. The conventional VRFB uses diluted H_2SO_4 as a support electrolyte. Support electrolyte is used for dissolving the vanadium ions and serves as one of the sources for proton production. The corresponding salts formed between vanadium ions and sulphuric acid can be found in (Table 6)[4].

Table 6. Concentration changes and vanadium ion salt formation during charging and discharging operation in both half-cells. (Blanc C., 2012)

Ion	Salt	Concentration (charging)	Concentration (discharging)	Half-cell
V^{2+}	VSO_4	Increases	Decreases	Anolyte
V^{3+}	$V_2(SO4)_3$	Decreases	Increases	Anolyte
VO^{2+}	$VOSO_4$	decreases	Increases	Catholyte
VO_2^+	$(VO_2)_2SO_4$	increases	Decreases	Catholyte

As it can be seen from the Table 6, at different stages of operation, different amounts of sulphuric acid interact with vanadium ions. For 1 M of vanadium ions between 0.5 and 1.5 M of sulphuric acid is required. Surplus of sulphuric acid in the electrolyte increases probability that vanadium ion will find its pair fast enough. Therefore, generally, the concentration ratio of vanadium ions to sulphuric acid is 1:2.

At fully discharged state the catholyte and anolyte contain only VO^{2+} and V^{3+} ions respectively. As the battery is being charged, the concentration of products goes down while VO_2^+ and V^{2+} ions are formed in the half-cells. This means that the reaction involving sulphuric acid concentrations for the anolyte becomes:

$$V_2(SO_4)_3 + 6H^+ \rightarrow 2VSO_4 + 4H^+ + H_2SO_4 \qquad \textbf{Equation 2-15}$$

For the catholyte, it becomes (involving water and sulphuric acid):

$$2VOSO_4 + 2H_2O + 4H^+_{acid} + H_2SO_4 \rightarrow (VO^{\cdot}_2)_2SO_4 + 4H^+_{water} + 2H^+_{acid} + 2H_2SO_4 \qquad \textbf{Equation 2-16}$$

It can be seen from the two reactions above that for anolyte proton concentration goes down from 6 M to 4 M while in catholyte it goes up from 4 M to 6 M. This means that the electrolyte charge in two half-cells is out of balance and the battery might stop functioning due to high internal resistance build up. The PEM solves the problem by allowing excess protons to transfer to the other half-cell, thus keeping the two cell's charges equal in sign and magnitude. Christian Blanc has been able to analyse the situation analytically and empirically and he concluded that proton concentration in the cell is not

constant and it decreases as the battery is discharging and increases as it is charging[4]. The changes in proton concentration at different SoC may potentially serve as a SoC monitoring method. See Figure 16 for charging process chemistry, Figure 17 for proton concentration changes.

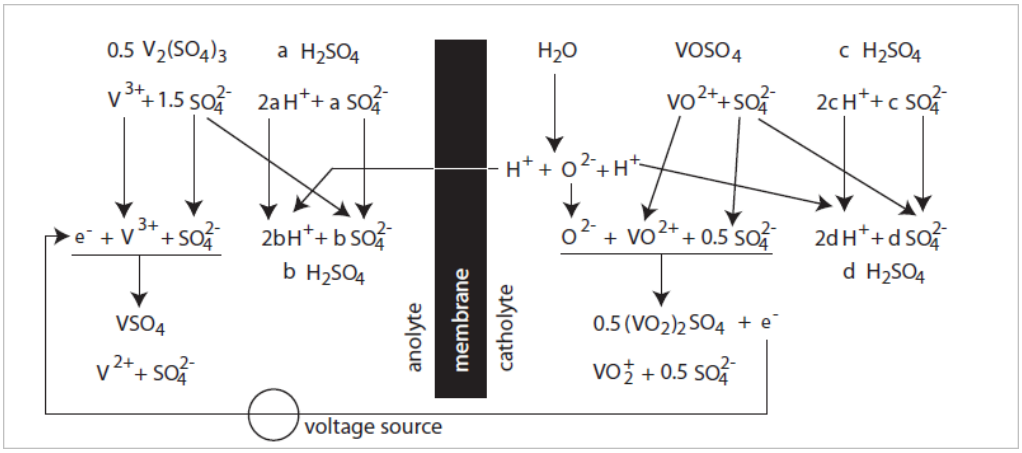

Figure 16. Full equation of battery charging process. Due to water dissociation in the catholyte, one proton is used to balance cathode reaction and one proton travels across membrane to balance anode reaction. (Blanc C., 2012)

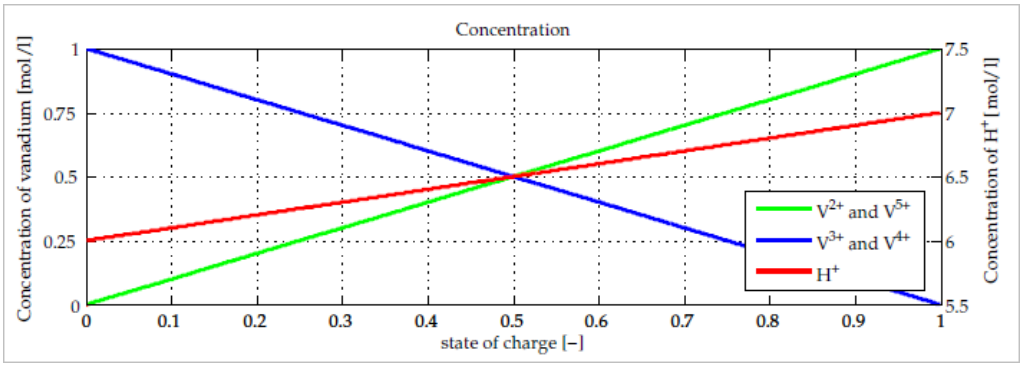

Figure 17. Depending on the SoC of the battery, concentration of protons in the system varies linearly; calculations done assuming 1M concentrations and standard conditions. (Blanc C., 2012)

Vanadium solubility is low in acid solutions especially in powder form, which makes electrolyte production an area of extensive research and stands as a barrier for VRFB commercialization. A lot of effort has been put into research of electrolyte dissolution methods since 1984. One of the first to address this problem was Skyllas-Kazacos and her research group[5, 6, 10, 26]. Initial attempts to directly dissolve vanadium in sulphuric acid resulted into 0.1 M concentrations, which did not provide sufficient energy density. Skyllas-Kazacos proposed to break electrolyte preparation into few steps. The general idea was to combine direct dissolution method with electrochemistry or with reducing agent. Depending on the method employed, electrolyte was either ready to be used or required additional charging. In any case, most of the methods allowed reaching concentrations as high as 2 M. Some of the most known and used methods will be discussed below.

- *Vanadium Pentoxide dissolution using reducing agents*[10]

The V_2O_5 is cheap source of vanadium that can be obtained from industry as a by-product, which makes it very attractive for electrolyte preparation and gives potential

for system cost reduction. The V_2O_5 is added to sulphuric acid on a stirring plate and reducing agent is added. Reducing agent can vary depending on cost, safety and purity requirements. Typically, oxalic acid or sulphur dioxide are used as they leave no traces and are relatively easy to obtain. The vanadium pentoxide powder starts to dissolve slowly in the sulphuric acid, turning into VO_2^+ ions:

$$V_2O_5 + 2H^+ \rightarrow 2VO_2^+ + H_2O \qquad \textbf{Equation 2-17}$$

The VO_2^+ ions then react with reducing agent in acid environment, oxalic acid for instance; note that oxalic acid breaks down into water and carbon dioxide that do not contaminate electrolyte:

$$VO_2^+ + H_2C_2O_4 \rightarrow VO^{2+} + 2CO_2 + H_2O \qquad \textbf{Equation 2-18}$$

Oxalic acid can not reduce vanadium to V^{3+} state due to low electronegativity, however. Other reducing agents such as SO_2 may be used if needed. Having VO^{2+} ions is not enough as it only corresponds to catholyte in discharged state. The way around this problem is to divide VO^{2+} electrolyte into three equal parts by volume, load two volumes into the battery and apply voltage. The redox reaction will start leading to reduction of VO^{2+} to V^{3+} in anolyte and oxidation to VO_2^+ in catholyte. VO_2^+ is then replaced by a third volume of VO^{2+}. In this way V^{3+}/V^{4+} redox pair is obtained which corresponds to VRFB at 0 SoC. Alternatively, the volume could be divided into two and more violent reducing agent could be added to second volume to get V^{3+}/V^{4+} pair.

- *Vanadium Pentoxide dissolution using electrochemical methods[10]*

An alternative to reducing agent is to use direct current between anode and cathode. Many designs of electrode and cell have been developed for this method over past decades. The general procedure is somewhat similar for all methods. The V_2O_5 is placed into sulphuric acid on a stirring plate and the carbon electrodes are inserted at voltage of around 1.8-2 *V*. The vanadium powder starts to slowly dissolve in acid solution. The liquid form of VO_2^+, when comes in contact with anode might get reduced to any oxidation state between V^{2+} and V^{4+}. If V^{2+} and V^{3+} ions are formed, they react with V^{4+} and V^{5+} ions when come in contact or get oxidized if collide with cathode. Further procedure depends on the cell structure. Some designs complement cell with reducing agents to speed up the process and shift reaction reduction, some place PEM between electrodes and fill cathode side with pure sulphuric acid to avoid oxidation of ions. Depending on design of cell, end product can be V^{3+}, V^{4+} or even a 50/50% mix of those ions, also known as $V^{3.5+}$. In any case, further electrolyte preparation steps are done via VRFB charging just like in section above.

- *Vanadyl Sulphate dissolution*

This is by far the simplest, fastest and most precise method available to date. The raw material costs much more than in methods above, however, which makes it economically infeasible for mass production but an option for laboratory scale. Vanadyl sulphate ($VOSO_4$*nH_2O) is purchased in powder form, added to sulphuric acid supporting electrolyte and stirred. The vanadyl sulphate readily dissolves in Sulphuric acid within few hours compared to few days duration in methods above. To speed up the process ultra-

sound can be used. After dissolution is over, two-step charging protocol needs to be carried out just like in methods above and the battery can be used after that.

- *Other methods*

There are much more exotic or industrial scale solutions to electrolyte preparation. A clever method of mixing V_2O_5 and V_2O_3 powder of controlled particle sizes in the sulfuric acid was proposed[4]. Some research groups use other salts of vanadium as a starting material such as ammonium. Cell configuration that allows in-situ electrolyte preparation was reported. Different supporting electrolyte compositions such as hydrochloric acid can be used to produce electrolyte with a bit different properties.

- *Verification of electrolyte SoC and purity*

At various stages of electrolyte production and battery operation there is a need to check whether the powder has fully dissolved, if the desired concentration has been achieved and whether there are any contaminants present. There are many possible ways to analyse electrolyte from simple visual inspection to sophisticated optical measurements. The first and simplest method to check whether desired electrolyte was made is to dilute the sample with water until it becomes transparent enough to shine light through. For 2 M vanadium concentrations, 10x dilution gives desired result. Looking at color gives an idea of which ions are dominating in the electrolyte (see Figure 15). In order to check whether any solid particles remain in the electrolyte a beam of light can be shined through after shaking the storage bottle, which is also called Tyndall test. In case if beam shines through without visible scattering, conclusion can be made that there are no solid particles inside. In order to determine correct concentration of certain vanadium ion in electrolyte, UV-Vis spectroscopy test can be done. UV-Vis spectrometer is a device that transmits light of UV-Vis range (200-800 nm) wavelength through the reference sample and the sample of interest and records how much of the light has been absorbed or transmitted in the process. It then uses data to plot absorbance values versus the wavelengths. Intensity loss that is experienced in reference sample is extracted from intensity loss at sample of interest. Generally, the solvent is placed in the reference sample so that its absorbance in the UV-Vis range does not interfere with absorbance of the compound to be analysed. Beer-Lambert-Bouguer law can be applied to find the concentrations of the samples:

$$A = \log_{10}\frac{I_o}{I} = \varepsilon l c \qquad \textbf{Equation 2-19}$$

Where A is absorbance, I_o is intensity at reference sample, I is intensity at the sample of interest, ε is extinction coefficient $\frac{L}{Mol \times cm}$, l is the path length or length of the cuvette (cm) and c is the concentration of chemical compound (M). The UV-Vis analyser shows as an output how much light has been absorbed on the scale from 0 to 5, where 0 corresponds to 0%, 1 to 90%, 2 to 99%, 3 to 99.9% light absorbed and so on. It is much easier to analyse samples with absorption between 0 and 3, so dilution of the samples is one of the simple ways to go. Alternatively, sample holders with smaller path length could be used.

The spectrometer outputs the value of absorbance at given wavelength. The path length is normally 1 cm and ε is a constant for given chemical compound at given wavelength. It can be found by analysing series of samples of known concentrations or from literature. Once ε has been determined, concentration of ions can be found by simple rearrangement of equation. The concentration of ions is directly related to the SoC of the battery. During battery operation, knowing exact SoC is of high importance as it allows automating battery control systems. A lot of effort is put into research of SoC monitoring currently[18, 19, 27]. Some groups report that UV-Vis is potentially a viable option for the task but problems such as spectra overlap occur with catholyte half-cell[5, 27].

There are other methods being developed for SoC monitoring. It was mentioned that heat conductivity in both half-cells varies linearly with changing SoC. Using the conductivity meter one can correlate the readings to electrolyte's SoC. The problem with the method is that for each set up new calibration needs to be done. Alternatively, one could use potentiometer to monitor potentials of both half-cells and then, using Equation 2.5 and 2.6 determine the SoC of the battery. The data is inaccurate, however, due to self-discharge, oxidation of anolyte and migration of water. Both Nernst equation and conductivity measurements are simple tools for manual inspection but are not yet sufficient to be automated to monitor the SoC of the battery. UV-Vis, on other hand, has potential for automated control as it can both check concentrations of species in both half-cells and correlate graphs to SoC.

3 EXPERIMENTAL

3.1 Safety considerations for VRFB operation

Safety is one important factor to consider when working with VRFB. The following table summarizes what constitutes potential danger in VRFB and how to prevent the mishaps.

Table 7. Safety considerations when working with VRFB.

Danger	*Potential event*	*Risk level*	*Prevention measures*
Sulfuric acid	Spill, skin/eye contact	High	Use of PPE, testing battery for leakage before using
Vanadium powder	Inhalation, skin/eye contamination	Medium	Use of fume cupboards, careful handling
DC power supply	Short circuit, electric shock	Low	Accurate and sensible handling of equipment
Tubes and connectors	Leakage, disconnection due to high pressure	Medium	Use of correct connectors, decreasing pumping speed and hence the pressure in tubes
Scalpel knife	Slight-deep cut on the skin	Low - Medium	Careful handling of instruments

3.2 Electrolyte preparation and monitoring

Major part of the electrolyte preparation and monitoring investigation was done during the summer work and detailed information about experiments, alternative preparation methods and additional findings can be found in summer work report. List of reagents used in the following experimets is summarized in the Table 8.

Table 8. Reagents used for production of electrolytes.

Reagent	Purity	Supplier	Manufacturer
Divanadium Pentoxide	99.6 %	Sigma-Aldrich	Sigma-Aldrich (Austria)
Sulfuric acid	95.0-98.0%	Sigma-Aldrich	Sigma-Aldrich (Germany)
Oxalic acid dihydrate	> 99.5%	Merck	Merck (Germany)

After careful screening of existing vanadium compounds that could be used as a starting substance for electrolyte preparation, vanadium pentoxide (V_2O_5) was picked for its high vanadium mass to molar mass ratio and low price compared to other compounds. Best choice would be to pick vanadyl sulphate powder and use direct dissolution method as stated in section 2.5 but due to high material cost and its low supply in Finland it would turn out into unreasonable expenses and long waiting times. On the bright side, vanadium pentoxide, which supplies V^{5+} ions, allows doing additional dissolution and precipitation experiments.

The work started by testing whether V_2O_5 is really almost insoluble in diluted sulphuric acid. Five beakers containing 100 mL 4 M H_2SO_4 were placed on stirring plates with Teflon coated magnetic rod placed inside. Doses of V_2O_5 were added to each plate such that vanadium ion concentrations would comprise 0.05, 0.1, 0.15, 0.2, 0.25 M respectively. The stirrers were closed with lid to prevent liquid evaporation and left for a cou-

ple days to mix. At the end, all the beakers were inspected visually and with light scattering test to see if any powder remained in the solution. The solutions were also taken for UV-Vis analysis to log characteristic peaks of obtained VO_2^+ (V^{5+}) ions.

- Sample dilution and UV-Vis analysis

In this work, all of the samples that were taken to UV-Vis were diluted by a factor of 10. The same factor allowed easy comparison of spectrums of electrolytes obtained at different stages of work. The dilution was done right inside the cuvette. The cuvette volume is 3 mL, so 300 µl was left for electrolyte and 2700 µl for solvent (water). The 1 mL micropipette was used to fill the cuvette with water and 100 µl pipette was used to add the electrolyte. The electrolyte could be released from pipette only when the tip was submerged in water, so that no spontaneous reaction would happen between electrolyte and atmosphere. The 1 mL pipette was then used for mixing the solvent and electrolyte inside the cuvette to obtain homogeneous solution. In cases when electrolyte was checked during the battery operation, a small portion of electrolyte was extracted right out of the working storage tank using a syringe and stainless steel needle.

All samples were analysed in UV-Vis spectrometer in absorbance mode. Before doing the analysis, spectrometer would be turned on and left to heat up for 30 minutes to let the bulbs pick up the intensity. Baseline was then scanned. In cases when samples were analysed every few hours, baseline would be scanned every time before starting new measurement batch. The reference cuvette contained deionized water. The spectrum range was picked from 950 to 300 nm and scanning speed of 400 nm/min. After scanning the sample, the spectrum was sent to analysis, the cuvette extracted from machine and cleaned with deionized water.

- Stock electrolyte production and concentration verification

Next step was to try different V_2O_5 reduction and dissolution methods to obtain VO^{2+} (V^{4+}) ions. Two options to do that, as stated is section 2.5, are by means of electrochemistry or with help of reducing agents. In case of electrochemical dissolution, 500 mL of 4 M H_2SO_4 was placed on the stirring plate with magnetic rod in the beaker. Anode and cathode rods made from carbon were placed into the solution and connected to power supply at 1.8 *V* (1.25 *V* for redox reaction and 0.55 *V* extra to overcome overpotentials). The lid was sealed with Parafilm to prevent evaporation of water over time. Since only two electrodes were available at the time, it was decided to add V_2O_5 in portions such that vanadyl sulphate concentration starts at 0.1 M and goes up to 2 M if possible. Every new portion was added when it was clear that all powder from previous batch has fully dissolved.

In case of reducing agent, oxalic acid was chosen as it was available in the lab at the time and was relatively inexpensive substance to use. Additionally, in the reaction oxalic acid breaks into CO_2 and H_2O and hence leaves no traces in the electrolyte. Due to high accuracy of the method, it was reliable for determination of extinction coefficient of vanadyl sulphate. Determination of coefficient using UV-Vis required a few samples with varying concentration. Five beakers with 100 mL of 4 M H_2SO_4 were placed on

the stirring plate. V_2O_5 and $H_2C_2O_4$ was added to each beaker such that final concentration of solutions would correspond to 0.05, 0.1, 0.2, 0.3 and 0.4 M. The beakers were labelled accordingly, sealed and left to mix for a few day until no traces of vanadium powder were detectable visually. Next, the samples were taken to the UV-Vis spectrometer, diluted 10 times and analysed in the 220-900 nm wavelength range. The dilution of samples decreases vanadium ion concentration and hence decreases absorption caused by the solution. Once the data was collected in form of Absorbance vs wavelength graphs for each sample, characteristic peaks could be found for the electrolyte. Absorbance values were taken at the same wavelength, preferably peak, and correlated between each other. Values of absorption at picked wavelength were plotted versus the concentration of given solution. When the points were connected, the obtained graph resembled a line, the slope of which is the extinction coefficient.

After determination of absorptivity of coefficient, it was possible to prepare stock electrolyte ($VOSO_4$) of known concentration. The concentration was decided to be 1.8 M as it is low enough to avoid precipitation of vanadium salts from solution and yet high enough to extract comparable to other research groups amount of energy. 800 mL beaker was placed on a stirring plate with oxalic acid and V_2O_5 in a proportion to obtain 1.8 M stock electrolyte that could be then used in RFB to charge the battery.

- Nafion 117 membrane preparation

Most of the further experiments require RFB station to be set up. To be able to operate RFB station, the membrane needs to be activated. Commercially available Nafion membranes are not ready to be used as PEM right away. The pores in the membrane act as a size exclusion mechanism, letting only molecules of few small radius through the membrane. Before using the membrane, it has to be pre-treated to become activated. The negatively charged end-groups act then as a repulsive barrier for anions. The preparation of Nafion membrane includes the following steps:

- Cut membrane sheet to desired geometry.
- Place the membranes into 3 wt% hydrogen peroxide solution for 1 h at 60 °C.

The peroxide serves as a cleaning agent, killing any bacteria and dissolving dirt from the membrane surface.

- Take membrane out from the peroxide bath, rinse it in boiling deionized water and put it to boil in another beaker for 15 min. Repeat the procedure two more times.

The water needs to be deionized; it is best to have six beakers of boiling water ready.

- Place membranes into 1 M sulfuric acid solution at 75 °C for 2 h.
- Repeat the cleaning procedure with water three more times.
- Store membranes in cold deionized water with a closed lid to prevent any contamination. The storage time should not exceed 2 months.

- First charging step using RFB (obtaining V^{5+}/V^{3+} pair)

Since dissolution using oxalic acid only produces V^{4+} ions, two charging steps are required for the preparation of battery at fully charged state. In first step the stock electrolyte was placed into both anolyte and catholyte storage tanks. The RFB station was assembled as shown in Figures 18 and 19.

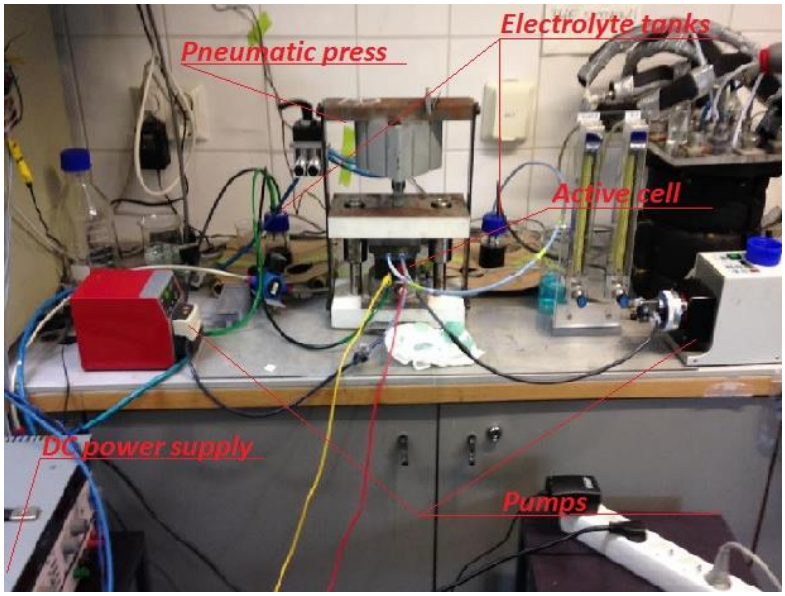

Figure 18. RFB system after adaptation from DMFC test station

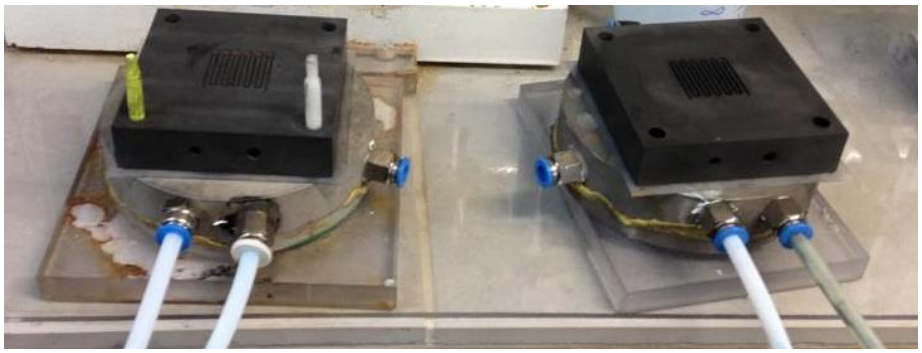

Figure 19. RFB reaction centre. From bottom to top: PET endplates, aluminium flow guide plate, silicon gasket, graphite plate, guide pins.

Rubber gasket was placed over endplates. O-rings were inserted into graphite plates, which then were carefully placed on the gaskets using PE rods as guide pins. GDL was placed over the serpentine channels of graphite plates. The PEM was placed between graphite plates such that O-rings create airtight seal with membrane when compressed by pneumatic press. The cell was then placed into the press and tubes from anolyte and catholyte were attached to half-cells. After the RFB station was assembled, pumps were turned on and DC power supply at constant 1.6 *V* was connected to the cell. Anolyte tank was also connected to nitrogen loop to avoid contact with air and possible ion oxidation. The electrolytes were pumped through the cell and were periodically taken for UV-Vis analysis. Extraction of electrolyte was done using a syringe in order to avoid oxidation of anolyte and not to stop battery operation. The samples were then diluted to

10% of initial concentration and analysed using UV-Vis until formation of ~1.8 M V^{5+} in catholyte and V^{3+} in anolyte was confirmed. The visual inspection of electrolyte reservoirs was done frequently. The anolyte should become emerald-green and catholyte should turn yellow while stock electrolyte is blue. The V^{5+}/V^{3+} pair does not correspond to battery in neither charged nor discharged state. For that reason V^{5+} was replaced by V^{4+} electrolyte so the battery corresponded to its fully discharged state of V^{4+}/V^{3+} pair. The leftover V^{5+} solution could either be disposed or recycled. Both methods are described separately later.

- Second charging step using RFB (obtaining V^{5+}/V^{2+} pair)

After obtaining V^{4+}/V^{3+} pair, the battery can be charged further using the same set up as in second charging step with 1.8 *V* supply to achieve V^{5+}/V^{2+} pair, which corresponds to fully charged battery. The anolyte should be taken special care of as it rapidly oxidizes in presence of air. Oxygen and hydrogen gas formation in the anolyte also affect the anolyte, so it requires frequent purging by inert gas such as nitrogen. During charging procedure, samples were taken and analysed using UV-Vis until formation of ~1.8 M V^{5+} in catholyte and V^{2+} in anolyte was confirmed. The extinction coefficient of V^{2+} at 800 nm, as reported by Skyllas-Kazacos is 2.415 $\frac{L}{cm*M}$ and it was used for monitoring of V^{2+} concentrations[28]. The colour of V^{2+} ions is violet, so it can also be visually inspected.

- Disposing or recycling of V^{5+} leftover solution.

In order to minimize environmental contamination by vanadium, leftover electrolyte was heated up. At elevated temperatures V^{5+} is unstable and vanadium starts to precipitate from solution. Liquid part was then drained by dilution and leftover vanadium powder stored into powder waste.

To save money in addition to minimizing waste, electrolyte was reduced back to V^{4+} state with help of oxalic acid. The resulting $VOSO_4$ electrolyte was analysed with UV-Vis spectroscopy until recycled electrolyte spectrum matched the initial stock electrolyte spectrum. Once the spectra matched, recycled electrolyte could be added back to stock electrolyte container and reused in further experiments.

- Battery discharging using RFB (obtaining V^{4+}/V^{3+}) pair

Once the battery was fully charged, discharging could be done to collect data for efficiency and battery capacity determination. Discharging set up was similar to the one used in charging, except for instead of power supply, load was used. The battery was connected to load source that was controlled by a direct methanol fuel cell (DMFC) software. Although DMFC software was designed specifically for fuel cells, its basic functions could be used for simple battery discharging while still getting data output. During discharging samples from catholyte were taken to UV-Vis until formation of 1.8 M $VOSO_4$ of blue colour was confirmed. Additionally anolyte was checked using UV-Vis to see if it was discharging at the same rate as catholyte. Another indicator that the battery was discharged was significant current output drop over time. When current

reached low values, it was evident that few reactive ions are left in the system, and it was concluded that SoC was close to 0%.

3.3 Mechanical design and cell stability

One of the main objectives of summer work was to build a functional RFB system with adequate mechanical design from scratch. Soon after careful evaluation of system components and requirements stated is section 2.4, it was concluded that it is possible to redesign already existing DMFC test station into VRFB. The DMFC consisted of one electrolyte storage tank, one pumping unit, heat control system and the reaction centre identical to the one stated in section 2.4. Therefore, the notable difference for RFB from DMFC was use of two electrolytes for extraction of energy and reversibility of the chemical reaction - DMFC can only supply energy while RFB works as both energy supply and storage. There were extra requirements for the cell such as proper sealing of electrolytes from contact with air, nitrogen loop and electrolyte leakage prevention.

The final cell assembly (see Figure 18) consisted of the following components:

- Two pumping units calibrated to produce 20 mL/min electrolyte flow speed. First pump was a "flow through" Ismatec pump taken directly from DMFC test station and second pump was peristaltic "Watson Marlow" pump taken from other project. Ideally, both pumps needed to be of the same type to provide best results but due to financial limitations this set up was used.
- Two electrolyte tanks - 200 mL glass beakers with screw lids. The catholyte reservoir had two drilled holes in the lid for electrolyte inlet and outlet. The anolyte reservoir required proper sealing from air contact therefore it had four holes combined with adjustable silicon insulators (See Figure 19). The first two holes were used as electrolyte inlet and outlet and the other two holes were connected to nitrogen gas supply, which is used to purge reservoir of any unwanted gases.
- Clamping unit - a pneumatic press that keeps cell in constant compression during operation. This component remained unchanged from DMFC set up.
- Two graphite plates - unchanged component from DMFC station. Ordered from FuelCell Store with dimensions of 74x74x18 mm, 6.25 cm^2 active area (see Figure 19).
- Sealing components. The silicon sheet was used between aluminium and graphite block with holes cut precisely at inlet and outlet locations. When compressed, works as a good seal. The gasket material (see Figure 12 for location) inside the reaction centre varied from set up to set up - ETFE film, Parafilm and Teflon sheets were mostly used.
- GDL - 140 μm thick carbon paper P75 ordered from FuelCell Store.
- PEM - Nafion 117 membrane ordered from FuelCell Store.

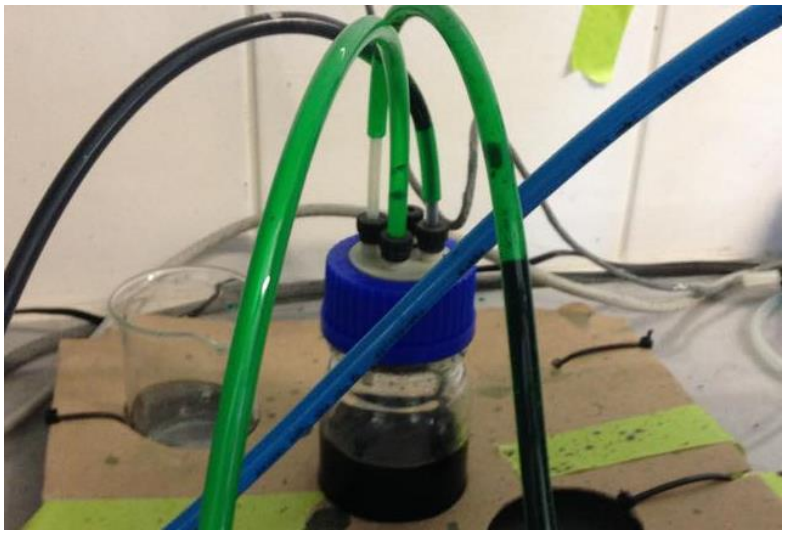

Figure 20. Final version of anolyte storage tank with insulated lid and extra nitrogen inlet.

Although the system built in summer was functioning, there was a number of design flaws with respect to RFB requirements, namely:

- Electrolyte leakage at aluminium plate - graphite plate junction and across the gasket in reaction centre.
- Unreliable lay-up of GDL-PEM-Gasket in reaction centre leading to imbalance in cell reactions, crossover of vanadium species and shifting of critical components.
- Some gasket materials such as Parafilm were compressed too much into the graphite plate and could only be removed with scalpel, leading to degradation of graphite.
- Immobility of the system due to fixed components such as the Pneumatic press.

The above-mentioned issues gave clear message that improvements or new design were required for further investigation of RFB. Due to time and financial limitations such factors as workload, material cost, design complexity and end quality improvements needed to be compared. Cells used by other research groups were screened to find inspiration for the design. The common difference from RFB built at Arcada was mobility of the system - instead of using pneumatic press, many research groups used plastic end plates and screws to keep the cell together[12, 14, 19] (see Figures 21, 22). Very little is said about professional cell designs, especially the sealing methods. It can be seen in Figure 21 from the blue stains on wood that hand-made cells seem to leak. Therefore, it was decided to try to design mobile cell that would resemble one shown in Figure 22 and to rely on expertise of Arcada university laboratory staff when seeking for proper sealing and tube connection solutions.

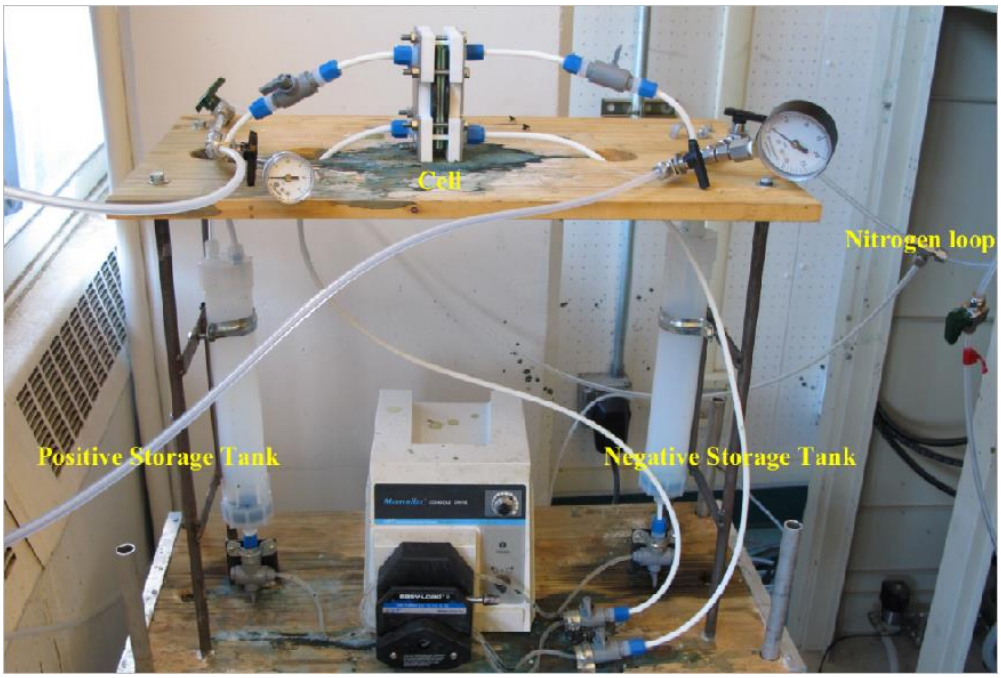

Figure 21. RFB system design made by Ya-Ching Tseng[12].

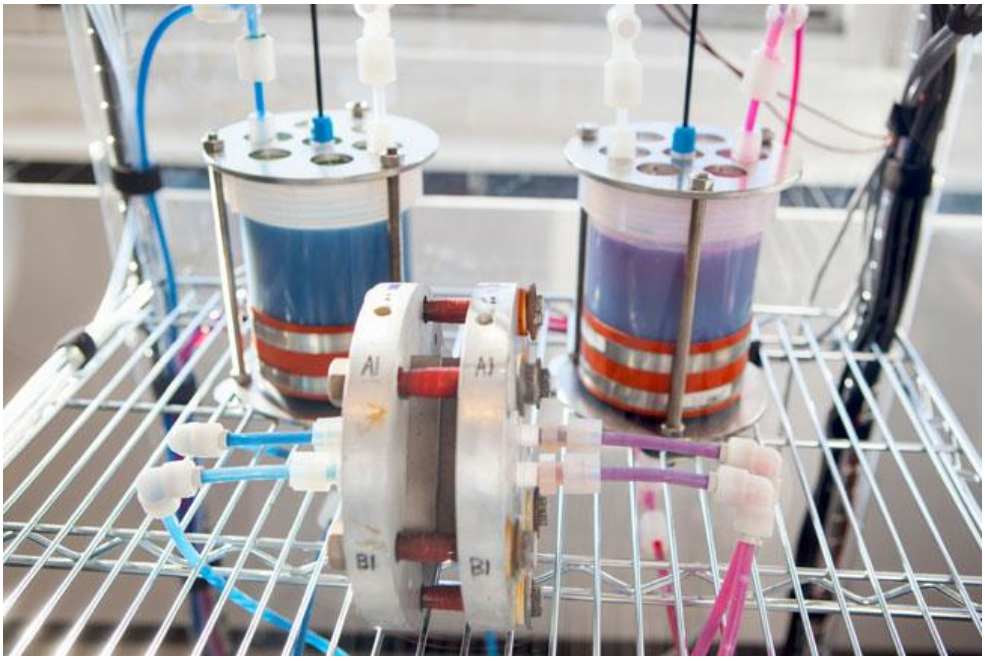

Figure 22. RFB reaction centre designed by research group of Michael Azis - the graphite plates are clamped between two circular aluminium end plates[14].

In the new design used in this study, the only component that could not be replaced due to high material costs was graphite plate; therefore, all cell components were developed from the graphite plate's dimensions. The graphite plate was functioning well in the old design - the only problem was gasketing of the graphite-membrane junction to prevent electrolyte leakage and crossover. Since different types of films did not provide required results during summer it was decided to mill a groove around serpentine flow channel.

In the groove, O-ring seal is placed, which, when compressed would firmly hold the membrane and allow no leakage. The design of graphite plate with O-ring can be seen from Figure 23.

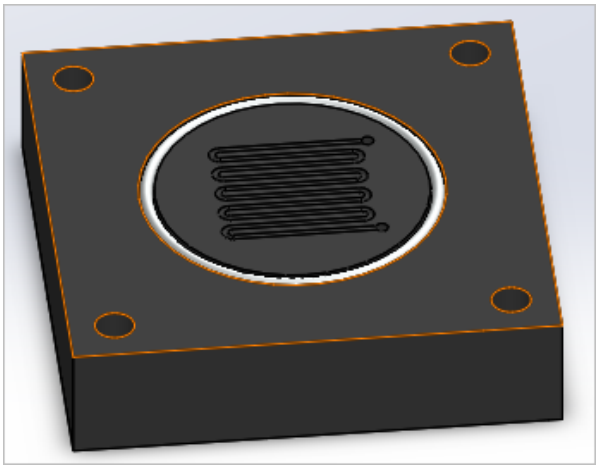

Figure 23. Graphite plate with O-ring around flow channel design. .

The O-ring sealing methods are numerous and there exist many guidelines for picking correct sizes of O-ring and groove for various situations. This case is static axial seal because O-ring lies in plane of junction and is not in contact with moving parts. Milling of the aforementioned grooves requires special tools for graphite - durable steel with diamond coating. Graphite is very hard and brittle material, so instead of removing chips from material, dust is extracted. In order not to break the plate, very slight depth increments are required and 20000 RPM was suggested for the milling. The groove's inner diameter was chosen to be 40.8 mm in order to avoid damaging the flow channels when milling and yet not to make O-ring too large. Knowing the inner diameter of the groove, inner diameter of the O-ring could be found. In this application, the ring is stretched a bit in order to firmly hold on to the groove and not to fall off. This suggests that in relaxed state ring's diameter could be found from the following formula[29]:

$$Ring's\ internal\ \emptyset = \frac{Groove's\ internal\ \emptyset}{\%\ elongation\ desired/100 + 1} \qquad \textbf{Equation 3-1}$$

The design guides suggest that O-ring stretch should not exceed 5% as any further stretch may cause drop in sealing performance. Assuming the stretch is 2%, the inner diameter of ring becomes $\frac{40.8\ mm}{1+0.02} = 40\ mm$. For 2 mm thick O-ring, the groove depth needs to be smaller by a factor of ring's desired compression. The compression for static loads can be within 10-40% depending on material chosen. The groove's depth was calculated using following formula[29]:

$$Groove's\ depth = \frac{O - ring's\ thickness}{1 + factor\ of\ compression} \qquad \textbf{Equation 3-2}$$

For compression of about 20%, and ring thickness of 2 mm, groove's depth becomes 1.7 mm. It is suggested that ring's cross-section should not exceed 90% groove's cross-section[29]. This is an easy check of the design feasibility. Assuming 70% is desired, groove's width could be calculated. Area of O-rings cross-section is $A_1 = \pi r^2 =$

3.14 mm^2. Therefore, groove's area becomes $A_2 = \frac{A_1}{0.7} = 4.48\ mm^2$ and width becomes

$\frac{A_2}{groove's\ depth} = \frac{4.482}{1.7} = 2.7\ mm$. The values are compatible with manufacturer's suggestion.

The material selection for O-ring depends on temperatures, load modes and chemical nature of environment. FPM (Fluorine rubber) material was suggested by manufacturer for applications involving acids. Similarly, small O-ring at endplate-graphite inlet junction was expected to enhance further the stability of the cell. This case is also static axial seal, but with a much smaller radius and instead of holding by extension, ring is kept in place by compression against the pocket walls. Pocket is better idea to mill rather than grove as ring would naturally take up all unwanted volume in the pocket. When squeezed it would leave space only for the electrolyte flow channel. In old design, square rubber gasket with small holes was used instead of O-ring. When compressed the holes were supposed to coincide with graphite inlets and form a seal. It did not work perfectly due to shifting of gasket, its wear over time and dirt on the surface (See Figure 24 below for comparison of old and new junction designs).

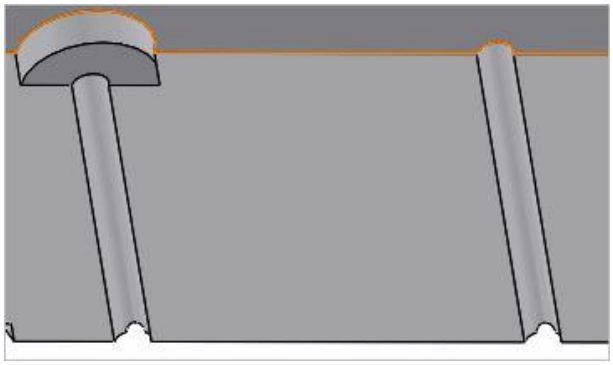

Figure 24. Endplate - graphite inlet junction design. To the right is the old design for square gasket, to the left is design for the O-ring.

The pocket and ring sizes were calculated similarly to first case. The ring's thickness was picked to be 1 mm and inner diameter 1.15 mm. The 0.8 x 3.12 pocket was then milled around inlets.

Next, the clamping plate of semi-circular form was designed from low density PE (polyethylene). The sidewalls are made vertical to make manufacturing stage easier as it is much easier to clamp parallel walls. Initial design had tapered walls, however. All the screw holes are equally spaced between each other on a circle centred at graphite plate so that all plate edges experience equal pressure. The clamping plate has a pocket of the size of graphite plate inside, so that no misalignment can occur. The plastic plate has small flow channels precisely at the same spot as graphite plate does. Depending on design choice for endplate-graphite inlet junction, one of the sealing solutions could be used. Either a 2 mm thick silicon gasket is placed between graphite and plastic plate or small O-rings are placed around the flow channels. At the front side, clamping plate has 6 mm threaded holes for electrolyte tube connectors. (See Figure 25).

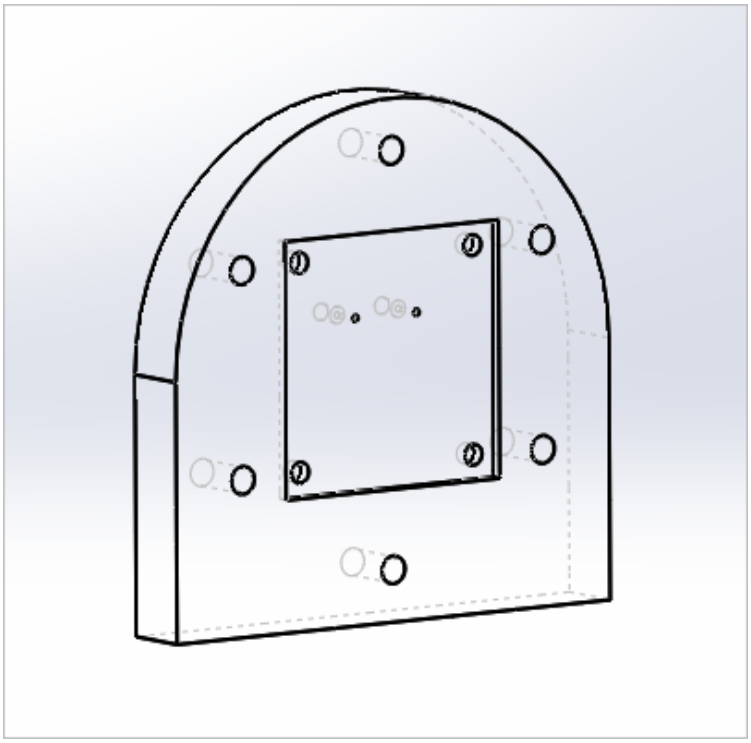

Figure 25. Clamping plate in-transparent appearance.

In both new and old design the alignment of two half-cells was achieved with use 6 mm thick guide pins that are screwed into the end plates. Due to wear and tear of old pins there was need to buy or make more of those. Therefore, polyethylene (PE) pins were made from PE sheet. The sheet was milled into 10x10x100 mm bricks. Then the bricks were placed into lathe and a rough cut was made on one side. That side was then used as a holder for the rest of the pin during lathing. The other side was drilled with centre drill and support was inserted into pin so that it does not deflect during lathing. Once set up, bricks were lathed and measured until outer diameter was approximately 6 mm. Since endplates have holes with M5 threads, one end of pin was cut to approximately 5.5 mm diameter. Thread maker was then attached to lathe and M5 thread was made on one end. The other end was lathed down to 4 mm in order to fit into upper endplate.

The full cell assembly would look as shown in (Figure 26). The carbon paper is placed on flow channels inside the O-ring groove and PEM is clamped between the graphite plates, resting firmly on the O-ring interface. The graphite plates are aligned with aid of chemically inert and nonconductive Teflon guide pins and clamped between plastic endplates by six screw connectors. For stability, the cell is placed into a pre-milled plastic plate that also has pockets for transparent electrolyte tanks. The tanks contain anolyte and catholyte respectively, which are fed into the endplates and attached to them by tube connectors (not shown in figure). In this way cell is mobile yet has little degrees of freedom, and cannot shift too much from desired position.

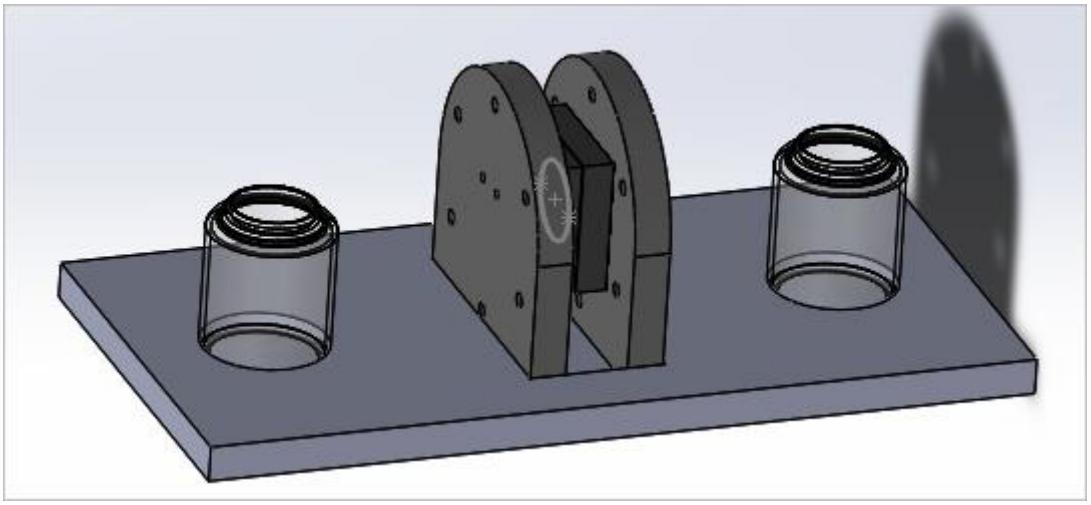

Figure 26. Design of the new cell test station.

After all the design work was done, existing system had to be evaluated against the new design to choose whether rebuilding is a better option than improving the system.

It was decided that no matter which system is used, the O-ring at graphite-membrane junction is a great solution to electrolyte leakage and cross contamination problem that also would significantly improve repeatability of component lay-up stage and prevent PEM and GDL from shifting during battery operation stage.

Table 9. Comparison table of existing and new design.

Problem	Solution for existing system	Solution for new system
Electrolyte leakage around PEM and shifting of components	O-ring sealing method	O-ring sealing method
Leakage at endplate - graphite plate junction	Replace square gasket with O-ring	O-ring connection
Mobility of the system	No solution due to presence of fixed components	The system can be moved around easily
Leakages due to poor pressure distribution	Change O-rings more often, increase clamping pressure.	Equally spaced screws around the cell should give reliable clamping force and pressure distribution
Electrolyte inlet/outlet channel design	Impossible to modify	Better than old system's design and tolerant to modifications
Time required	2 weeks	1 month
Expenses	Below 100 Euro	Below 100 Euro
Operation complexity	Medium	Medium
Implementation workload	Low	Medium

From the table above it can be seen that although it will take longer and requires more effort to build new system, it has potential to solve a number of problems that the old system can no longer tackle. Both systems would not cost too much to implement and both are not that hard to operate for a beginner. After careful evaluation, it was decided

to continue working on modifications to the DMFC station but to keep new cell design in mind for possible future development.

3.4 Battery performance characterization

Most of the experimental set ups for battery performance characterization are similar to the ones described in electrolyte monitoring section. The main objective of this work was to determine Coulombic efficiency of the battery along with its peak power to be able to compare against other research groups. In case if parameters matched the ones reported in literature, the test station could then be used for further RFB research. In case of poor results, the test station would require modifications to mechanical stability and/or sealing of electrolytes and reaction centre before it could be used for further research tasks.

- Determination of the peak power of the VRFB

The battery containing 30 mL of electrolyte on both sides was charged to 100% SoC as described in second charging step procedures in Section 3.4. The battery was then assembled and attached to DMFC software.. The DMFC was attached to a programmable load device, which was then attached to battery. The battery was turned on to pump electrolytes. The software was set up to start draining battery at 0.9 *V* and to decrease the load every minute by 0.1 *V* until load would reach 50 *mV*. The load would then return to 0.9 *V* and whole cycle would repeat until battery had fully discharged.

The voltage was set to be constant over the whole cycle. As the voltage decreased, the current was supposed to rise (Equation 2-4) but due to different overpotential modes coming in effect and SoC changes, the dependence was non-linear. The software recorded all the current-voltage data as a text file, which was analysed after discharge was complete. The power was found by multiplying current by voltage ($P = I \times V$).

The peak power is the highest value of all multiplications over the complete discharging period. The power curve was then plotted using Excel software to get a visual representation of how the battery behaves at different loads and SoC.

- Determination of VRFB's Coulombic efficiency

From Equation 2-7 fully charged 30 mL electrolyte contains:

$1.8\ \mathrm{M} * 0.03\ \mathrm{L} * 96485 \frac{C}{mol} = 5210\ C$ charge. This is the maximum value for discharging electrolyte to V^{4+}/V^{5+} state. However due to leakage, spontaneous reactions and other losses the value for discharging was expected to be lower than theoretical and value for charging process was expected to exceed theoretical value.

Determination of Coulombic efficiency is done via Equation 2-11:

$$\mu_{coulumbic} = \frac{\int I_{discharge} dt}{\int I_{charge}\, dt} = \frac{Q_{discharge}}{Q_{charge}}$$

Both data from charging and discharging of the battery needed to be collected. For discharging same set up as for peak power determination was used except for this time, the Voltage was kept constant at 1 V and the current was varying. The battery was discharged until SoC reached 0 and data was collected as a text file and imported into Excel for further analysis. Since the explicit formula for current behaviour during discharging is not known, the $\int I_{discharge} dt$ equation can be replaced by a less accurate but simpler summing operation: $Q_{discharge} = \sum_{t=0}^{i} I_t \times \Delta t$. The time fractions were the delays between data measurements, approximately 3-5 s.

The charging experiment was more complicated. The DMFC software can only be used to measure data during discharging experiments, as fuel cells cannot normally be recharged. All the hardware available at the time including power supplies, oscilloscope and multimeters had no data output ports or SD cards. Due to time and financial limitations, it was decided to go with a much simpler but less accurate solution. In the set-up, battery was left to charge just as described in Section 3.4, second charging step. A camera was attached to support in front of power supply. The camera was then programmed to take a picture of current readings every 30 s for infinite amount of times using "Lapseit" mobile app. Once the charging was completed, the camera was stopped and all pictures were imported to computer. The current readings from pictures were then manually entered in Excel and plotted versus time. Similar manipulations were done for finding $\int I_{charge}\, dt$ as in case of discharging. The dt was replaced by 30 s increments and the formula became: $Q_{charge} = \sum_{t=0}^{i} I_t \times \Delta t$.

From the results obtained, Coulombic efficiency was found and compared against the results reported by other research groups using similar components in the cell.

4 Results

4.1 Electrolyte preparation and monitoring

- Direct dissolution of vanadium in sulfuric acid.

Attempt to directly dissolve vanadium in sulfuric acid has proven to be impractical - the reaction turned out to be extremely slow stopping somewhere around 0.1 M concentrations of VO_2^+. Any undissolved V_2O_5 powder was filtered out with 20 μm filter paper and solutions were diluted with water to take for UV-Vis analysis. The VO_2^+ was hard to detect as it has distinctive peak at around 250 nm, where the UV-Vis machine loses too much information. Additionally, absorption coefficient is so high that only highly diluted samples could be detected. Some interesting peaks were found at around 228 nm. Yet, it was impossible to draw any conclusion whether it is characteristic peak for VO_2^+ ions, sulfuric acid or a phantom peak caused by machine settings. The experimental data was checked for matches in literature and it matched results of Skyllas-Kazacos' research group[28] (see Figure 27).

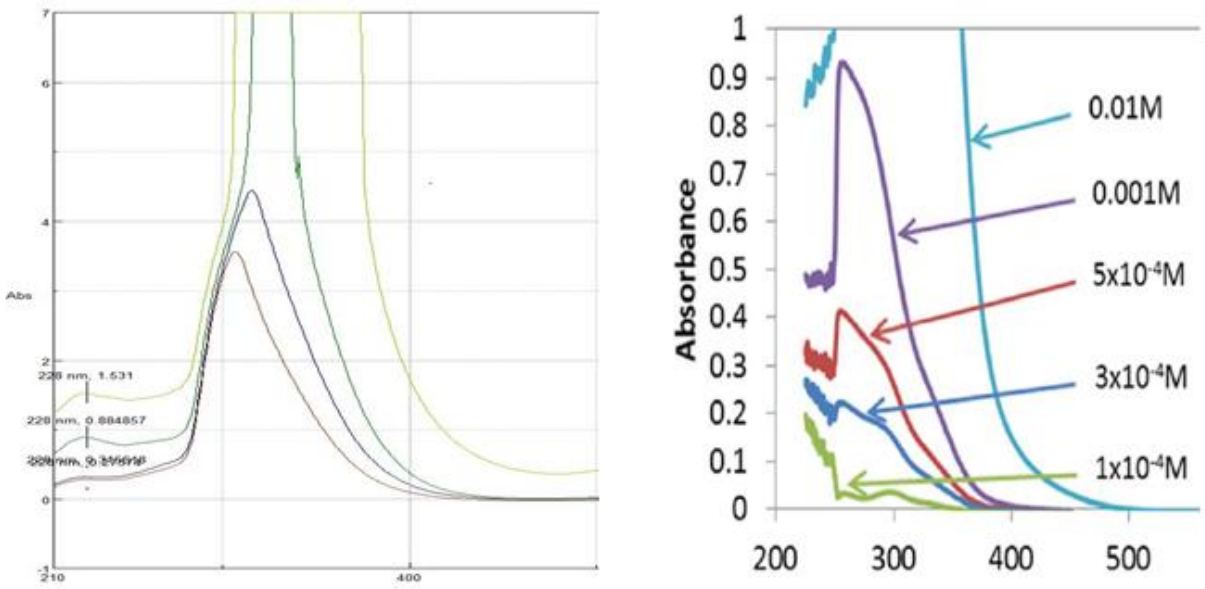

Figure 27. Comparison of results for UV-Vis spectrum of V^{5+} ions done at Arcada (to the left) and by Skyllas-Kazacos' group (to the right).

- Electrochemical dissolution and reduction of vanadium

During electrochemical dissolution experiment, soon as voltage was applied to the system, instantly there was bubble formation at electrodes and evolution of hydrogen gas. It was observed that while keeping voltage constant, making magnetic stirrer spin faster made current rise but degradation of electrodes made current drop. The concentration of vanadium in this experiment corresponded to 0.4 M $VOSO_4$. The reaction went much slower than expected and solution was left overnight to prepare. Next morning there was a very dense blue solution of V^{4+} contaminated with carbon black. The electrode had eroded and its conductivity had decreased dramatically. Attempt to filter the carbon black out did not give satisfactory results as some carbon residue was left in the solution. UV-Vis analysis did not provide any readable spectrum for this experiment as even

very dilute samples absorbed all light both in absorbance and in reflectance modes. The method had to be left out until higher quality electrodes were available.

- Dissolution and reduction of vanadium using oxalic acid

The initial dissolution experiments using oxalic acid were dissatisfactory – the expected dissolution and reduction time turned out to be too long. The solution was left to mix until no particles detectable by human eye were left in solution. During mixing, it was possible to observe formation of CO_2 bubbles at the walls of the beaker, so the oxalic acid was actually reacting and dissociating. The production of 0.4 M $VOSO_4$ took two days and instead of expected blue solution, light green was obtained. Although green colour corresponds to V^{3+} ions, the UV-Vis did not confirm initial assumption. Next morning, however, the solution turned blue. It was assumed that green colour was due to the fact that mix of blue V^{4+} and yellow V^{5+}ions produced green colour when mixed. Quick experiment with combining the aforementioned solutions together showed that indeed presence of V^{5+} ions makes $VOSO_4$ solution look green.

The produced $VOSO_4$ samples were taken for UV-Vis analysis every few hours until no difference between last few could be observed. It was then concluded that all powder had fully dissolved and all of the oxalic acid had reacted with V^{5+} ions. However, the difference between absorbance results was evident if samples were checked once a day. It was supposed that since electrolytes are water based, poor sealing could lead to evaporation of water and hence to increase in molar concentration of vanadium ions. After substituting beakers with properly sealed jars, no more difference in results was observed.

After confirming that oxalic acid can be used for production of $VOSO_4$ stock electrolyte, absorptivity coefficient of $VOSO_4$ needed to be found in order to be able to monitor electrolyte concentrations. The UV-Vis analysis of 0.1 – 0.4 M $VOSO_4$ samples showed that there is characteristic peak at 765 nm. The comparison against literature showed that Skyllas-Kazacos' group had found similar peak for $VOSO_4$ electrolyte[28] (Figure 28).

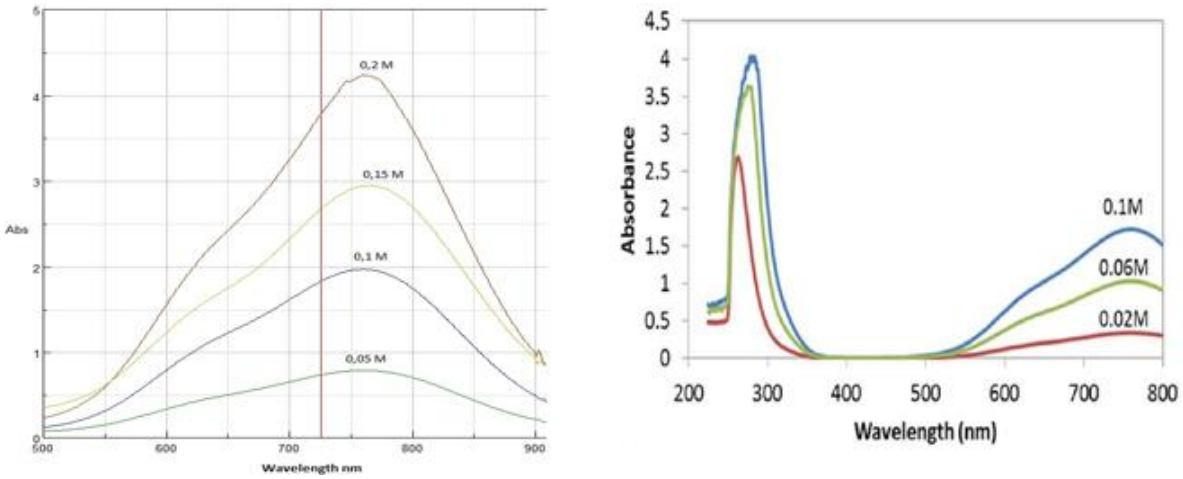

Figure 28. Comparison of results for UV-Vis spectrum of $VOSO_4$ done at Arcada and by Skyllas-Kazacos' group.

Plotting sample concentrations versus their absorbance at 765 nm produced a graph that showed strong linear dependency of absorbance on concentration. The slope of the line

was then found to be numerically equal to absorptivity coefficient. The coefficient was calculated to be 17.442 $\frac{L}{cm*M}$ at 765 nm, which is quite close to 17.166$\frac{L}{cm*M}$ at 760 nm reported by Skyllas-Kazacos[28] (Figure 29). It was then concluded that 1.8 M stock electrolyte corresponds to 3.24 absorptivity value at 765 nm.

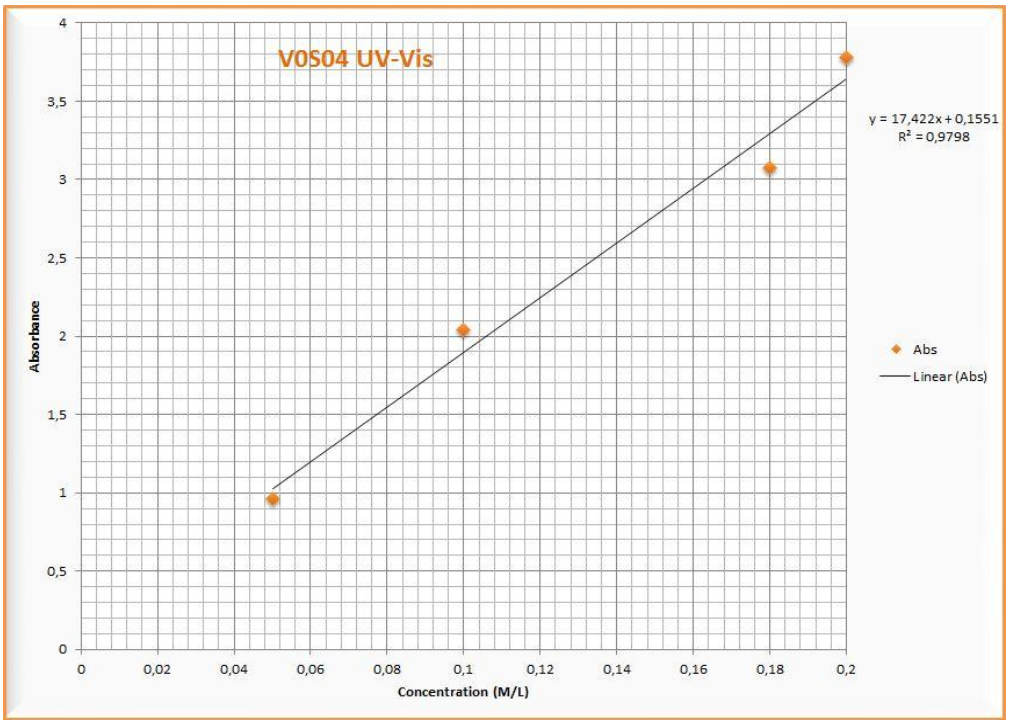

Figure 29. Determination of $VOSO_4$ extinction coefficient at 765 nm .

- Electrolyte monitoring during first charging step

Both catholyte and anolyte were charged simultaneously and periodically analysed at UV-Vis. The catholyte reaction was oxidation of V^{4+} to V^{5+} ions. As shown in Figure 27 there is no distinctive peak in the 180-400 nm region for V^{5+} ions but there is only one peak for V^{4+} ions containing solution. Therefore, an easy way to determine SoC of catholyte is to see how the peak of V^{4+} at 765 nm erodes from 3.15 Abs to ~0.2 Abs (Figure 30). Once the peak had disappeared, it was concluded that there are only V^{5+} ions present in the solution. In addition, the current readings suggested lack of reactive substances in the system. Initially, current was equal to 600 *mA* but as concentration of V^{4+} ions dropped, current also dropped to about 150 *mA* and stabilized there. Whole charging of 60 mL catholyte took around 11 h. See Figure 30 for graph of catholyte charging progress.

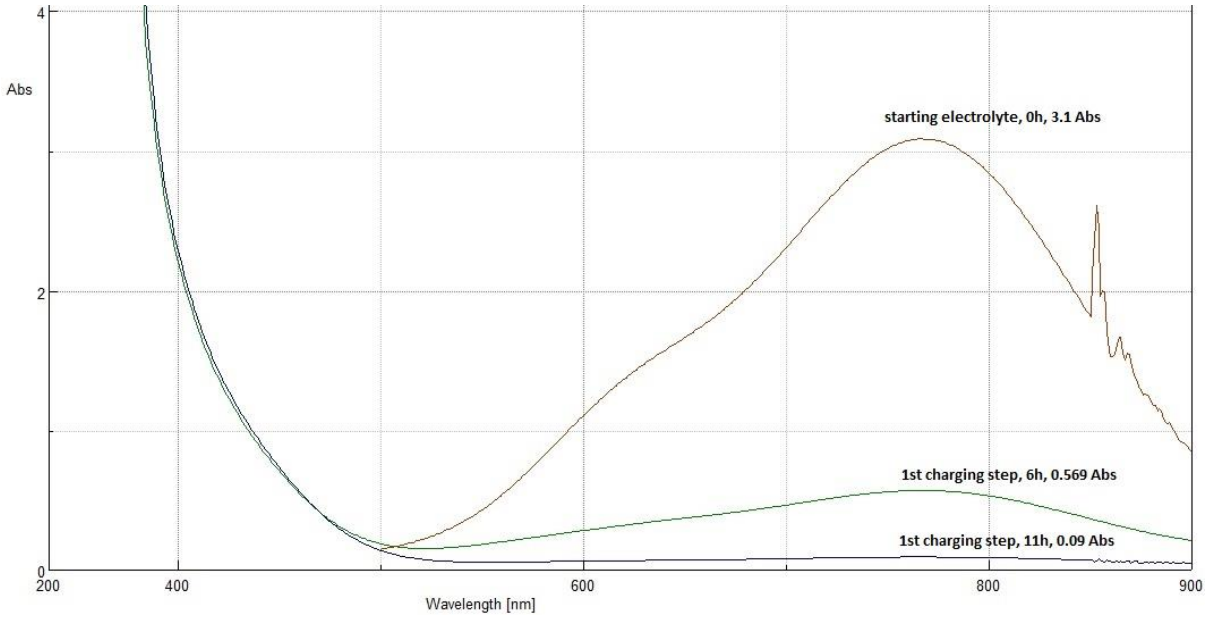

Figure 30. Charging of catholyte. As the concentration of V^{4+} ions drops, the peak at 765 nm erodes.

For the anolyte, SoC determination was not as straightforward. In theory, by the time the catholyte is fully charged, the anolyte should also be fully charged but it is not always the case. The reason for imbalance is due to ion cross-contamination, self-discharge and oxidation of anolyte due to oxygen formation at the anode. According to literature V^{3+} has characteristic peaks at 430 and 620 nm, which fully or partially overlap with V^{2+} peaks at 430 and 580 nm. V^{2+}, however also has a distinctive peak at 800 nm, extinction coefficient for which was found to be 2.42 $\frac{L}{Mol \times cm}$ by Skyllas's group[19, 28]. The following graph was obtained after 11 h of charging of anolyte (see Figure 31). The arrows show that as anolyte was charging, peak at 765 nm eroded to around 0.1 Abs and at 430 nm increased to approximately 2.3 Abs. Easiest way to conclude that 1st charging step for anolyte was completed was by looking at absorbance at 800 nm, where it should be less than 0.05.

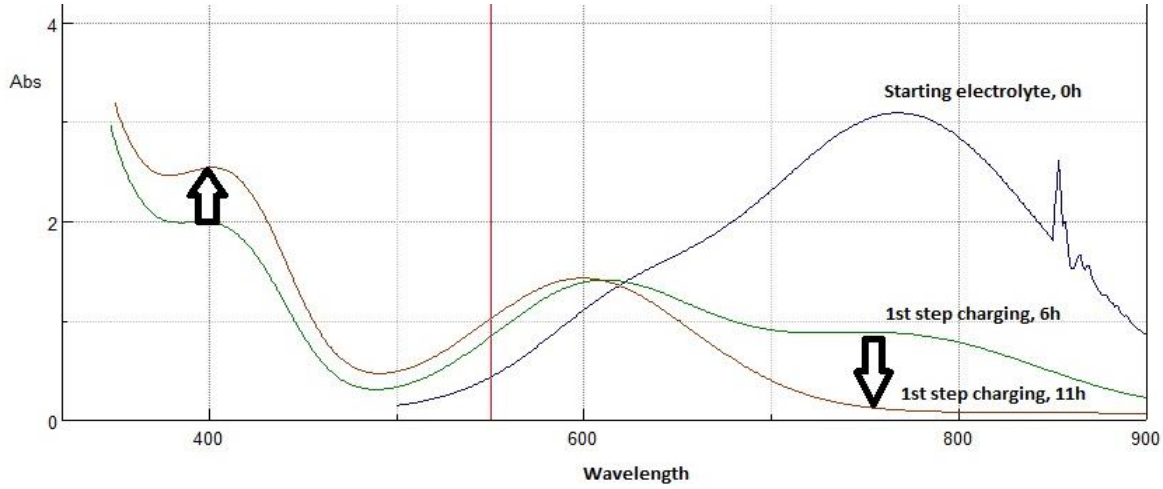

Figure 31. Charging progress of anolyte. The peak at 765 nm erodes as concentration of V^{4+} grows and peaks at 430 and 620 nm grow as V^{3+} ions form.

Anolyte was attempted to charge against a bigger volume of catholyte overnight at 1.6 *V*. As a result, a spectrum of pure V^{3+} was obtained (see red spectrum on Figure 31). The anolyte did not proceed to charge further into V^{2+} ions due to low Voltage supply. This method could be a viable option for preparation of V^{3+} electrolyte.

The results of first charging step of both catholyte and anolyte were compared against results of Skyllas-Kazacos' research group and no significant differences were observed[28] (see Figure 32).

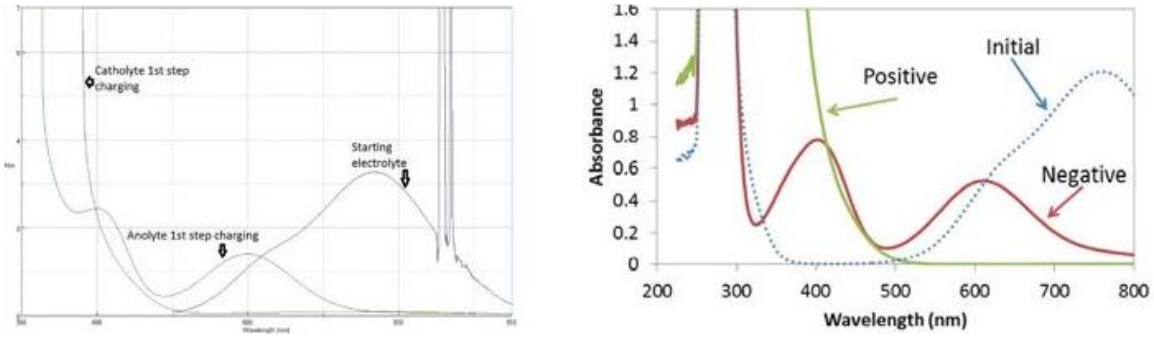

Figure 32. Comparison of first charging step's results at Arcada (left) and by Skyllas-Kazacos's research group (right).

- Recycling of waste catholyte

Waste V^{5+} ions were attempted to be recycled back into V^{4+} ions by use of oxalic acid as reducing agent. The samples were taken to UV-Vis for final V^{4+} concentration determination after 1 and 2 days of mixing. The stock $VOSO_4$ electrolyte had 3.15 Abs and the new electrolyte after first step charging following reduction with oxalic acid had 3.2 Abs. The values correspond to 1.8 and 1.81 M concentrations which was only a 0.1% difference. This difference could be caused by cross-contamination of vanadium ions or by slight evaporation of electrolyte during the battery operation (see Figure 33). The reduction reaction took less time to complete than during stock electrolyte preparation. This suggests that recycling of old electrolytes is more efficient than preparation of fresh electrolytes. Recycling of vanadium saved approximately 30% of material required for electrolyte preparation. Additionally it proved VRFB could be a more eco-friendly.

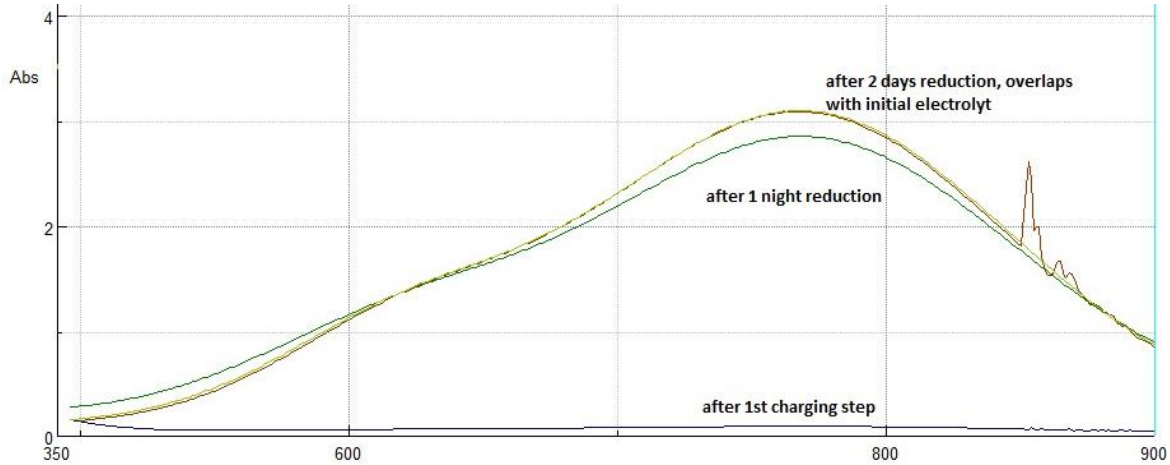

Figure 33. Recycling V^{5+} back into V^{4+} ions, initial and recycled electrolyte graphs overlap completely.

- Electrolyte monitoring during second charging step

Results for the catholyte UV-Vis in second charging step were precisely the same as in case of first charging step due to the fact that same stock electrolyte was used. The anolyte charging turned out to be a more complex task. By the time the catholyte was ready, same volume of anolyte was only half-way charged. To solve the problem, catholyte was stored in separate beaker and fresh $VOSO_4$ was used to aid in further reduction of V^{3+} to V^{2+}. The nitrogen purging was improved so that nitrogen loop would reach down to the bottom of anolyte tank and force out any dissolved gases from electrolyte. Due to electrolysis of water at anode side, spontaneous reaction was happening between V^{2+} and O_2 leading to self-discharge of the system. The voltage was increased to 1.85 V to overcome overpotentials and additional resistance caused by gas formation. The electrolyte flow rate was decreased to decrease pressure inside the cell. Improvements had an effect and the anolyte started to charge, changing colour from dark green to violet. UV-Vis analysis showed notable rise in absorbance at 800 nm. Similarly to Skyllas-Kazacos' group, it was observed that V^{3+} peaks at 430 and 620 nm start to shift to the shorter wavelengths, also known as blueshift, as concentration of V^{2+} grows[28]. See Figure 34 for progress in anolyte charging. The final sample had 0.43 Abs at 800 nm. Using the extinction coefficient found by Skyllas-Kazacos and Equation 2-19 we obtain: $C = \frac{0.43}{2.42} = 0.179$ M or 1.8 M for non-diluted V^{2+} electrolyte.

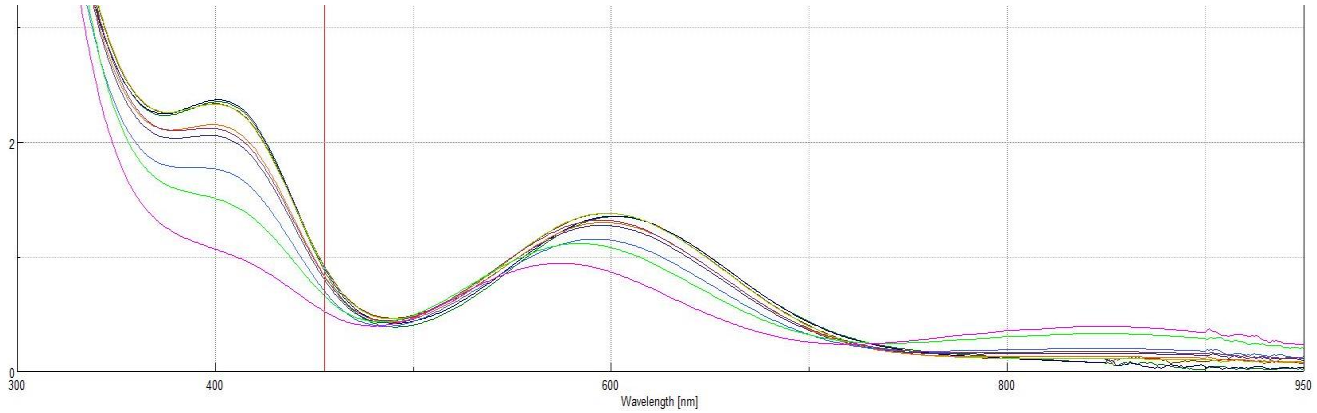

Figure 34. Charging progress of anolyte, purple spectra corresponds to fully charged state.

See Figure 35 for spectrum of fully charged battery.

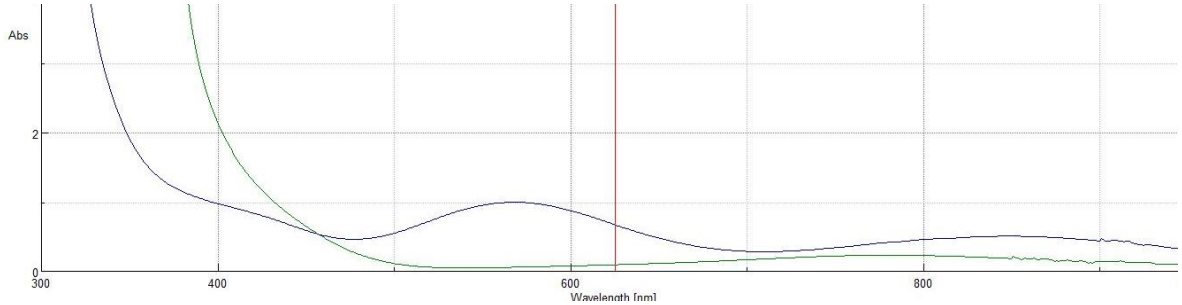

Figure 35. Spectrum of fully charged battery, containing V^{2+}/V^{5+} pair. The green curve refers to catholyte and blue to anolyte.

4.2 Improvements to mechanical stability

It was decided at the design stage that whether new cell or old DMFC test station was used, modifications needed to be done to the graphite plate. The graphite plate had two critical points where electrolyte leakage occurred. One point, where most of the electrolyte would be lost was at plate - membrane interface due to poor gasketing solution. Second point was at inlet/outlet - plate interface due to poor sealing material design. Best solution to sealing was found to be the O-ring method, which required milling grooves in graphite plates.

Once purchased, FPM was left in 2M H_2SO_4 solution beaker for 24 h. No weight loss or gain was observed over the period, which meant FPM is stable in mildly acid environments. Once the milling of grove was done, ring was tested to match the surface. The ring stretched as desired and firmly held on to the groove even in upside down position. When compressed, the rings would fully come down into the groove, making two plates come in full contact with each other, as desired. Leakage test was done at the DMFC test station with the new ring design, straight plastic film instead of Nafion membrane and 100 mL water instead of electrolyte. The test was done only through lower half-cell at 35 RPM using the peristaltic pump. Liquid content was measured in the beginning and at the end of the experiment. In the old design, approximately 10 mL of water was lost per hour due to leakages at both critical spots. With the O-ring only around 3 mL/hour of water was lost. Additionally, bursting test was done to the cell with same set up but RPM slowly growing from 35 to 100. The old design would give notable leakage already at 60 RPM. No leakage was observed at maximum RPM pumping with the O-ring method.

After installation of smaller O-rings, both half-cells were left for 5 hours to pump water. No leakage was observed on the membrane surface. There was notable leak at smaller O-rings, though. After carefully polishing Aluminium end plates the leakage did not stop. It was observed that although O-rings compress against end plate, it comes partially in contact with plastic tubes that are used as flow guides in the end plate. Deflection of those tubes caused uneven compression in O-ring and eventual electrolyte leakage. Combination of the O-ring and silicon gasket have solved the problem. No leakage was observed for the last set up.

During set ups with Nafion membrane, however, some leakages were observed occasionally. Some set ups would leak less, some would not leak at all. The reason for that was uneven swelling of Nafion due to moisture uptake. In addition, during regenration step the membranes get heated up – the membrane swells towards the heating plate, especially at the edges. The problem of swelling and eventual leakages was solved by covering edges of lower graphite block by Parafilm, which would not let membrane shift and serve as an additional stopper, not letting O-rings crash entirely into the grooves. Some leakage was still observed after hours of operation but it was so tiny that it did not affect results significantly.

4.3 Performance of the battery

- Peak power determination

Peak power was analysed with a test system designed for DMFC testing. It turned out that software constantly switches between constant voltage and dropping voltage modes. The mode of interest was dropping voltage but it was second on the list. Since initially battery was subjected to a constant load, some of the charge may had been lost, which could have influenced the peak power calculations. The readings from peak power determination experiment of dropping voltage vs current were imported into Excel for analysis and the following graph was obtained (see Figure 36).

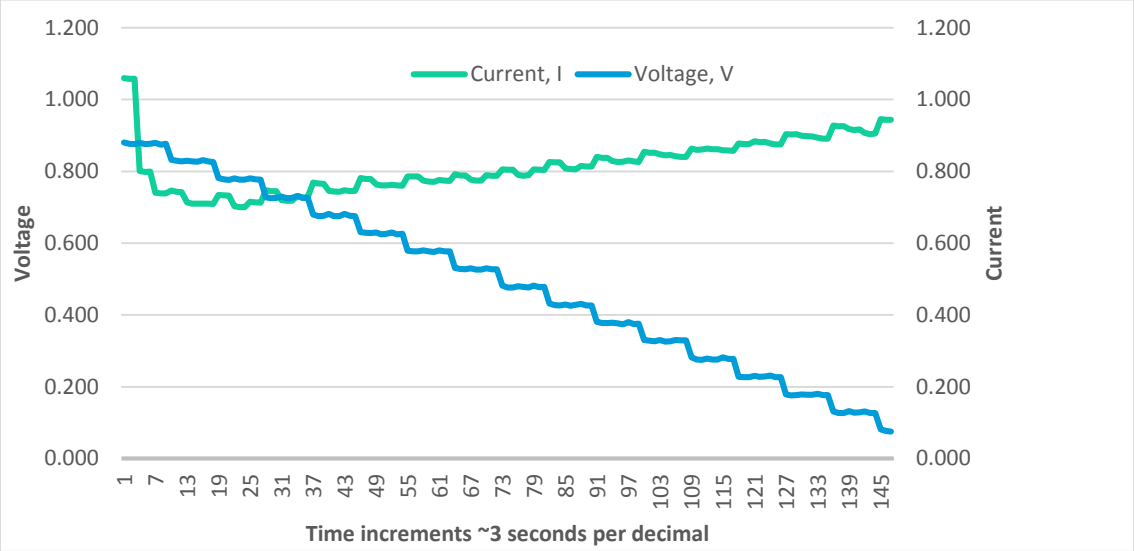

Figure 36. Dropping voltage mode during discharge, one polarization cycle.

It is evident from the graph that as the voltage was dropping by 100 *mV* current was rising by a value less than 100 *mA*, reaching 0.9 *A* at near short-circuit state. The instantaneous power was automatically calculated by multiplying corresponding voltage and current readings. The following graph was obtained (see Figure 37).

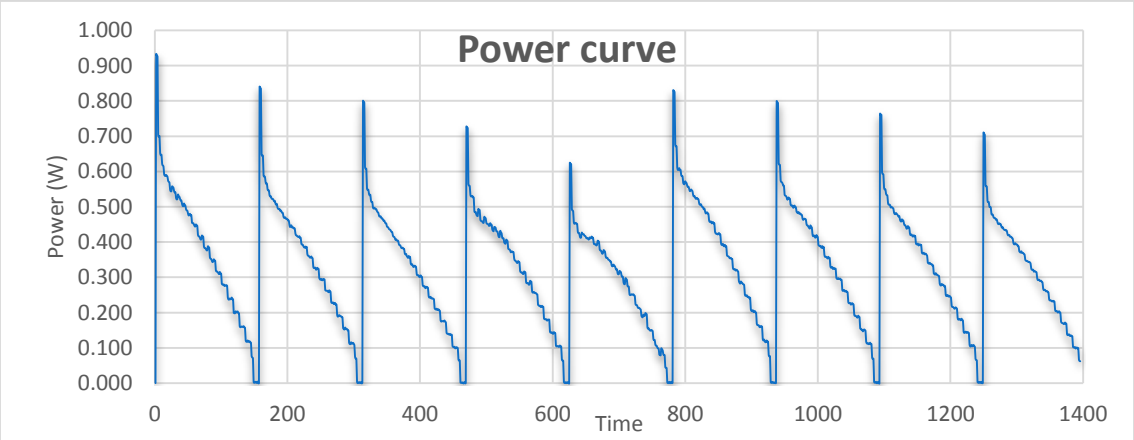

Figure 37. Power curve of nine polarization cycles.

It can be seen from the Figure 37 that as the discharging progressed and the SoC was dropping, the power output of battery was dropping. At "800" mark corresponding to 40 min on horizontal axis a significant rise in power output can be seen. In reality it was caused by shaking of electrolyte tanks, which improved mixing of fresh and already reacted electrolytes. The peak power during polarization was found to be 0.9 W or 0.15 $\frac{W}{cm^2}$. During normal operation, however, peak power was 0.7 W or 0.11 $\frac{W}{cm^2}$ corresponding to 900 *mV* and 800 *mA*. The commercially available VRFB are reported to deliver power in the range of 0.1 $\frac{W}{cm^2}$, which means the prototype had managed to reach commercially acceptable standards[30].

- Coulombic efficiency determination

During discharging experiment of 30 mL the data was automatically collected by DMFC software. The discharge period at 1 *V* load turned out to be 4 h. Initial current output started at 500 *mA* and, as the SoC was dropping, the current went down to 10 *mA*. The UV-Vis showed that anolyte had completely discharged while catholyte had around 0.2 M of V^{5+} ions left over. In all likelihood, imbalance was caused by spontaneous oxidation of V^{2+} ions in the anolyte. The current readouts were multiplied by time fractions of 3 s (time between measurements) and instantaneous charge transfer vs time plot was obtained. See Figure 38 for the discharge plot obtained from raw data.

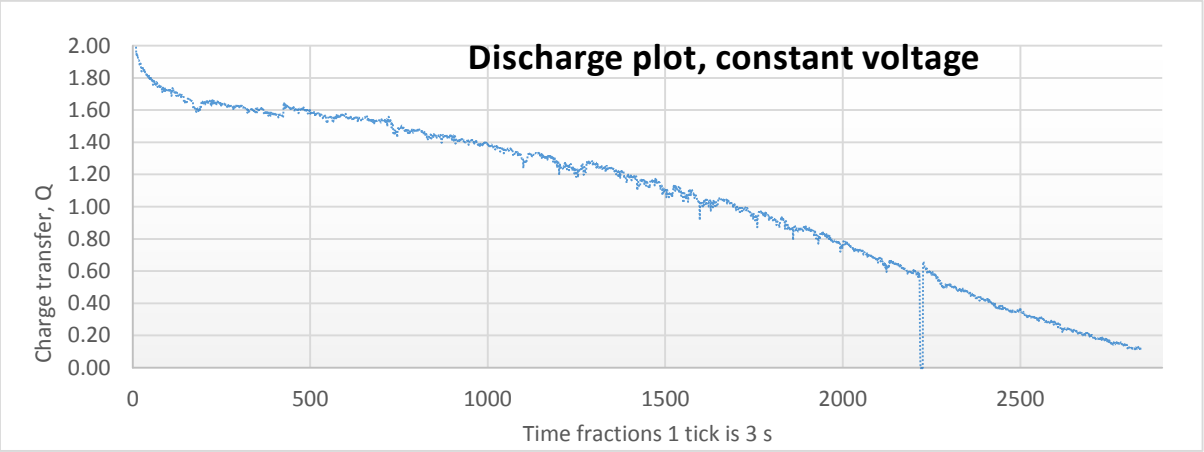

Figure 38. Discahrge plot of 30 mL battery at constant load.

No charge transfer can be observed around point 2300 (1 h 55 min) on the horizontal axis. This was caused by electrolyte measurement procedure, which required turning off both pumping units. Apart from that point, the trend is smooth enough and battery behaved like predicted - as concentration of reactive substance was dropping, less and less energy could be supplied to the sink.

The sum of all charge points corresponds to total charge transfer from the battery to the load. The sum then changes to Equation $Q_{discharge} = \sum_{t=0}^{i} I_t \times \Delta t$ into $Q_{discharge} = \sum_{t=0}^{i} Q_t$. The calculation using Excel software showed that total charge transfer was 3017 Coulombs, which is only 60% of theoretical maximum for this set up. The total discharging time was calculated to be 4 h.

The charging procedure was more complicated, as expected. The battery was plugged to charge right after discharging procedure ended to avoid any changes in SoC caused by external factors. The current supply started at 800 *mA* and was gradually decreasing until 200 *mA* over period of 4 h. The UV-Vis analysis showed that both anolyte and catholyte had charged to around 90% within 3.5 h and SoC reached a plateau. The problem was caused by eventual leakage of the battery, which reduced electrolyte composition at anolyte side by approximately 5 mL. The data was nevertheless obtained and plotted in MS Excel using same approach as with analysis of discharging data. The following graph was obtained by plotting charge transfer to battery (Q) versus time intervals of 30 s (see Figure 39).

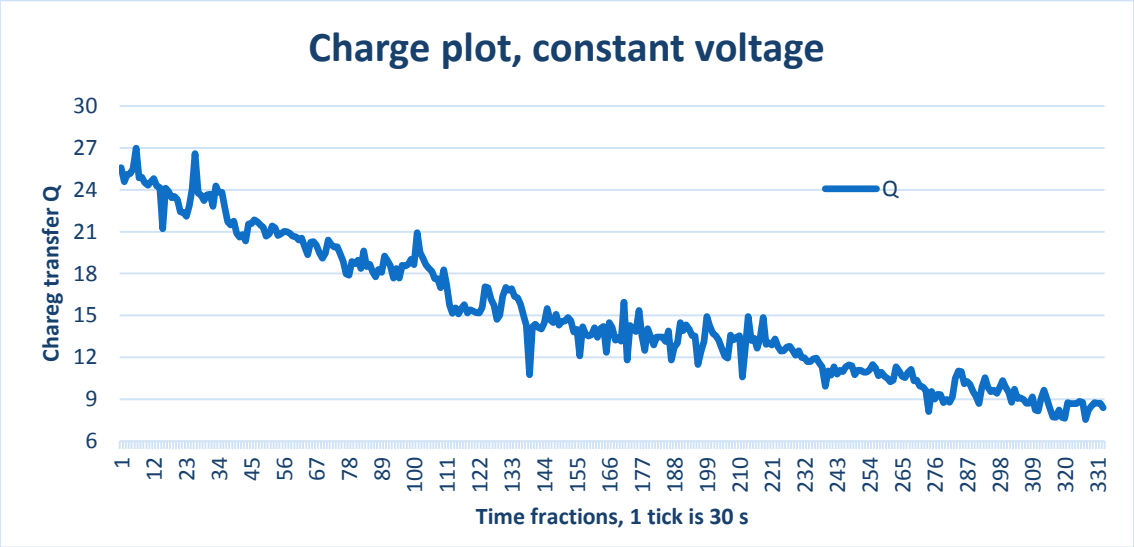

Figure 39. Charging plot of 30 mL battery.

Due to 10 times bigger data recording intervals the discharge plot looks less smooth. Still, calculating $Q_{charge} = \sum_{t=0}^{i} Q_t$ gives 5010 *C*. The value would have been larger if no leakage occurred. Also, this value cannot be treated as absolutely correct due to the fact for the last 30 min the SoC of the battery did not change.

Using available data, Coulombic efficiency can be found by dividing $Q_{discharge}$ by Q_{charge}, hence $\mu_{coulumbic} = \frac{3017}{5010} = 0.6\ or\ 60\%$. The obtained value is lower than efficiency reported by other groups ranging between 80 and 95%[5]. Highly possible that this low efficiency was caused by leakage and overcharging of one electrolyte side. The testing set up was well made but larger volume of electrolyte would provide much more accurate data as it would be affected less by leakages and imbalances.

5 Discussion

5.1 Discussion of the obtained results

5.1.1 Electrolyte preparation and monitoring

The literature and patents have been thoroughly reviewed for stock vanadium electrolyte preparation methods. Due to lack of detailed information, some of the methods were reconstructed through trial and error attempts. For economic reasons cheap source of vanadium metal was found and purchased in form of V_2O_5 powder. From many various dissolution attempts, only chemical reduction of powder was found to be repeatable, easily controllable and relatively safe to perform. The most reliable way to monitor concentration of prepared electrolyte was found to be UV-Vis. The extinction coefficient was found for $VOSO_4$ to be 17.442 $\frac{L}{cm*M}$ at 765 nm. The preparation method of the stock electrolyte from V_2O_5 powder is summarized in the flowchart below (see Figure 40). Systematic guide can be found in the lab notes and summer work report.

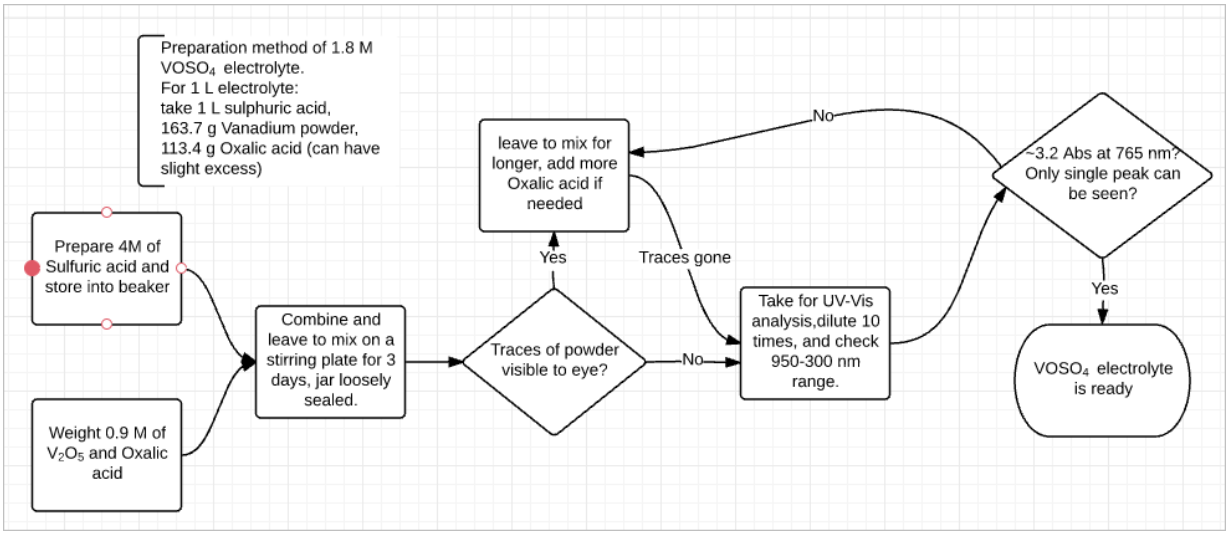

Figure 40. Flowchart of stock electrolyte preparation method.

Due to low supply of V_2O_5 powder in the laboratory, method of recycling used electrolyte was developed. In all likelihood, the method is not an invention but it is surprising how not a single reviewed publication except patents mentioned electrolyte-recycling methods. The recycling method allows saving approximately 30% of investments in raw material and reduces environmental impact of VRFB, making it a no-waste technology. In results section only V^{5+} to V^{4+} recycling was mentioned. V^{3+} is even simpler, however - bubble air through the electrolyte until it oxidizes to V^{4+} state.

Spectrums of all oxidation states of vanadium had been collected in the progression of this work (see Figure 41).

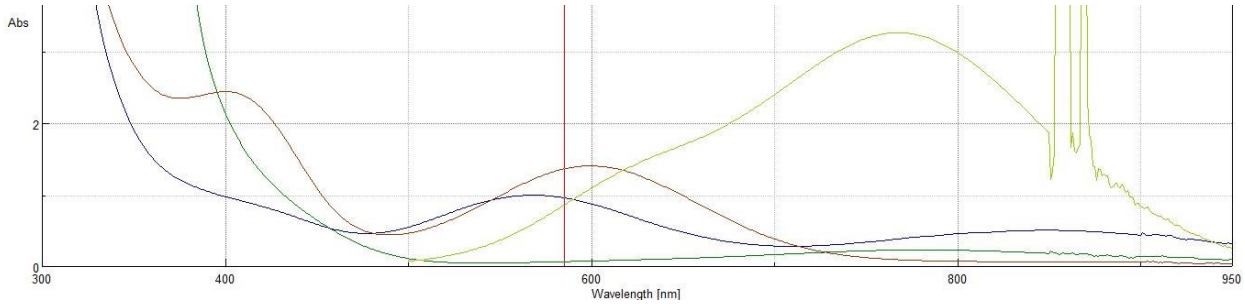

Figure 41. V^{2+} (blue line), V^{3+} (red line), V^{4+} (yellow line) and V^{5+} (green line) spectrums.

The spectrums were compared to the spectrums collected by other research groups using similar electrolyte compositions. The results matched with Skyllas-Kazacos' research group, meaning that the target of building a prototype and collecting vanadium in all oxidation states was achieved (see Figure 42).

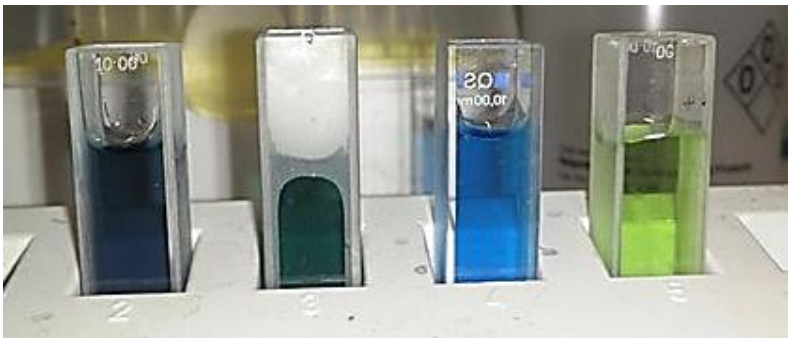

Figure 42. From left to right: V^{2+}, V^{3+}, V^{4+} and V^{5+} solutions. .

The analysis of catholyte side revealed that V^{5+} has no distinctive peaks in visible region but its concentration can be easily monitored through erosion of V^{4+} peak at 765 nm. The anolyte monitoring was more complex task due to overlap of peaks of V^{2+} and V^{3+} ions. Point at 800 nm was found to be a reliable indicator of anolyte composition. If no absorbance is present at 800 nm, the electrolyte contains V^{3+} ions mostly. If absorbance is present but the peak is shifted (760 -765 nm), then the anolyte contains V^{4+} ions in addition to V^{3+}. In case if a small peak at 800 nm and a bit bigger at 850 nm can be seen, the electrolyte contains V^{2+} ions with possible presence of V^{3+} ions. It was observed, that as concentration of V^{2+} ions increased, the peaks at 430 and 620 nm decreased and shifted to the left to 400 and 580 nm respectively. Extinction coefficient at 800 nm reported by Skyllas-Kazacos was used to monitor concentration of V^{2+}. It was verified that absorbance value of 0.43 at 800 nm corresponded to 1.8 M concentration of V^{2+} ions in non-diluted state.

5.1.2 Mechanical stability improvements

Notable electrolyte leakage during battery operation was addressed prior to start of this project. The solution was introduced in form of an O-ring that works as a seal on both sides of graphite plate. Although no leakage was observed with flat plastic sheets, the battery still leaked a bit when Nafion membrane was used. Possible cause for that is swelling of Nafion and therefore better sealing method is required or different membrane needs to be tested to eliminate any electrolyte losses during battery operation. The electrolyte leakage was stopped, however, leading to a much more stable system. Possi-

bly, a larger electrolyte volume needs to be tested with current set up to see if minor leakages will have effect on the results. Currently, extra layer of Parafilm was placed on the edges of lower graphite plate to catch Nafion membrane in place. The solution had improved sealing solution significantly but a more robust method needs to be developed still.

In progression of this work a step-by-step guide for battery set up and electrolyte charging was developed. The flowcharts below summarize corresponding guides (see Figure 43 and Figure 44).

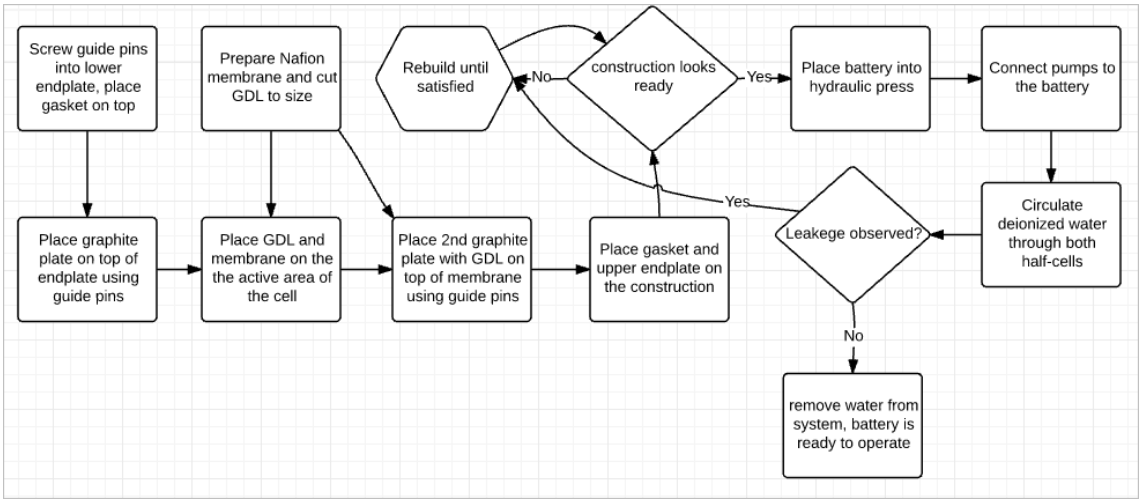

Figure 43. Battery set up flowchart.

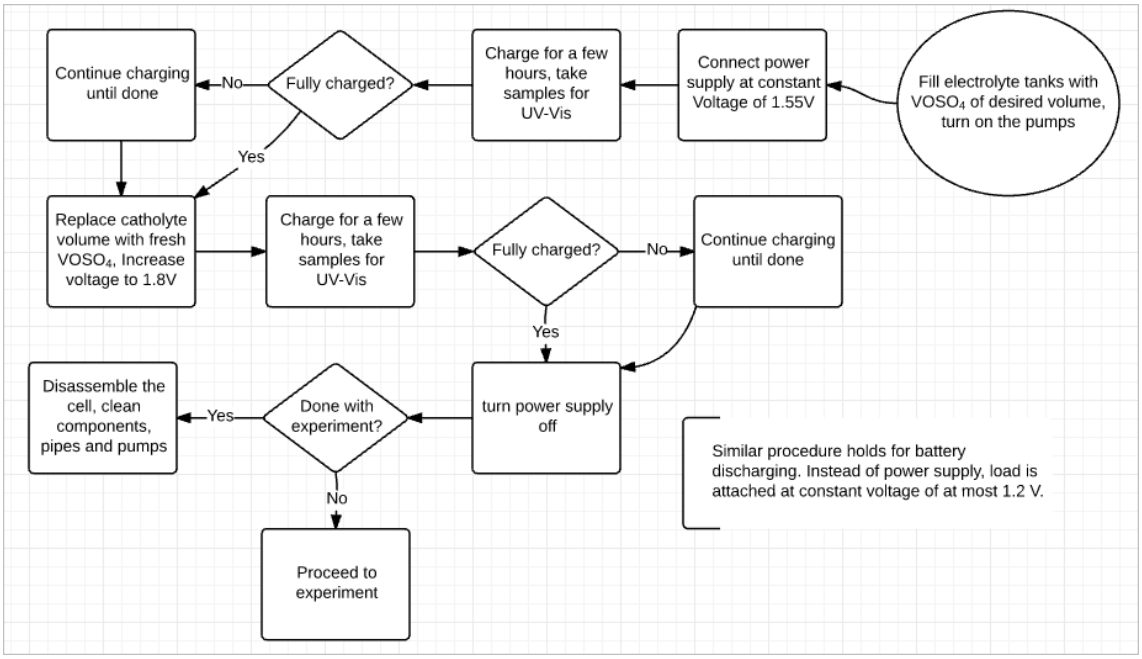

Figure 44. Battery charging/discharging flowchart.

Alternative cell assembly was designed to improve stability of the battery further. Due to time limitations, only a few critical aspects of design were implemented. The cell construction was left out as a suggestion for future work.

5.1.3 Performance of the battery

The performance of battery characterization was one of the more challenging tasks due to lack of testing hardware. DMFC testing system was adapted to record data during discharging operations and camera was used to record data output during charging of the battery. The peak power of cell was found to be 0.9 W or 0.15 W/cm^2 for the activation and 0.7 W at stabilized conditions. Further experiments with polarization at higher voltage need to be done to get results that are more accurate. At this stage, however, results seem to compile with data on commercially available VRFB set ups[30]. The coulombic efficiency of current set up was found to be 60%. Although 60% is an achievement for first attempt, it is below efficiencies of 90-95% reported by other research groups. More accurate testing of battery needs to be done with appropriate hardware. The measurement error from camera is approximately 6 times larger than using DMFC software due to the fact that measurement is taken 6 times slower. Additionally, the leakage problem needs to be addressed, as it is critical not to lose electrolyte during the charging process. To minimize damage to results caused by sample extraction and electrolyte leakages one should consider testing electrolyte volumes of around 100 mL or more. The testing time will increase but on the other hand, results that are more accurate can be found.

5.2 Recommendations for further work

This VRFB project is a potential foundation for further experiments and research in the area. There are plenty of opportunities for further development of the VRFB in areas such as mechanical engineering, material selection, chemistry, spectroscopy and electrochemistry. A list of topics that could possibly be of interest for whoever decides to take over the project is presented below.

- Test station design and manufacturing

The DMFC test station that was used for experiments with VRFB was not designed for VRFB. Many aspects, as discussed in "Methods" section could be improved. It is highly possible that replacing hydraulic press with more convenient clamping method could do the trick. One could further develop the new cell design presented in this work and proceed with manufacturing and testing of new cell.

- Battery performance characterization

The battery was charged and discharged a few times during this work. Evidently, the obtained results could be more accurate and repeatable. Development or purchasing of hardware suitable for RFB and other energy conversion systems such as DMFC would be of an advantage.

- Membrane modifications and performance in RFB

Nafion membrane has proven to work well in VRFB but many problems such as ion cross-over and membrane swelling arose. Screening of other available membranes and

modifications to Nafion membrane pre-treatment could be done to see if there are cheaper/more suitable options available in the market.

- Study on RFB behaviour with pre-treatment of GDL

GDL was reported to catalyze redox reactions between vanadium ions. Pre-treatment of GDL allows functionalizing it with end-groups, which could further improve reaction kinetics of vanadium ions[12].

- Electrolyte SoC monitoring

Although a lot of effort in this work was devoted to monitoring of electrolyte SoC using UV-Vis response method, many other methods exist that could potentially be simpler and faster. The electrolytes are reported to have changing proton concentration as the SoC changes, which makes it a potential way to use pH of electrolyte as an indicator[4]. In addition, the conductivity of electrolyte and OCV of battery change linearly with SoC, making them a viable option for SoC monitoring[28].

- Test other electrolyte compositions

The VRFB is only one of many energy electrochemical energy conversion technologies. Further research of metal and organic electrolytes should be done. Currently a lot of research is concentrated on development of new organic RFB such as quinone that could compete with metal-based systems[14].

- Build a demonstration renewable energy-RFB-load system

Demonstration system could be used as an educational battery for students. The use of diluted electrolytes would allow demonstrate how the SoC changes inside the battery as energy is converted from sun/wind into chemistry and is transferred to load (a fan or lightbulb). Apart from demonstration, the system would require redesign of the cell and planning of how to connect renewable energy technology to the battery.

6 Conclusion

A reliable preparation method for vanadium electrolytes to be used in an all-vanadium redox flow battery was established in the course of this work. An electrolyte recycling and rebalancing method was developed, which allows saving 30% of investments in raw materials during the electrolyte production stage. An electrolyte SoC monitoring method using UV-Vis spectrophotometry was also developed. The spectra of vanadium ions in all oxidation states were collected. Specific wavelengths were found for concentration monitoring of each oxidation state, which could then be directly related to the SoC of the battery. The results were compared against other research groups and were found to match their reported results. Other SoC monitoring methods were not investigated in this work and left for future possible projects.

The vanadium redox flow battery was modified to attain higher stability during set up and operation stages. O-ring grooves were milled around the active area and inlets of the graphite block. The amount of leakage decreased or was eliminated as a result. During prolonged operation, it was observed that small leakages still occurred due to membrane swelling and at graphite-endplate junctions. The battery set up and operation instructions were made to help future project workers in the assembly of the aforementioned cell. A improved design of a reworked VRFB test station was presented but not fully implemented due to time limitations.

Charging and discharging experiments of the VRFB were performed. As a result, the battery's peak power was found to be 0.9 W or 0.15 W/cm^2 and Coulombic efficiency 60%. More accurate results would require a better testing system than that available at the time. Electrolyte and cell stability also had an impact on results.

7 References

1. Electrochemical technologies for energy storage and conversion. Somerset, NJ, USA: John Wiley & Sons; 2011. ID: 10575560.

2. World energy outlook 2012. France: International Energy Outlook, IEA Publications; 2012.

3. New lens scenarios: A shift in perspective for a world in transition. Shell Global; 2013.

4. Blanc C. Modeling of a vanadium redox flow battery electricity storage system. Ecole Polytechique Federale De Lausanne; 2009.

5. Skyllas-Kazacos M, Chakrabarti M, Hajimolana S, Mjalli F, Saleem M. Progress in flow battery research and development. J Electrochem Soc 2011;158(8):R55-79.

6. Parasuraman A, Lim TM, Menictas C, Skyllas-Kazacos M. Review of material research and development for vanadium redox flow battery applications. Electrochim Acta 2013 7/1;101(0):27-40.

7. Electrically rechargeable redox flow cells. 9th intersociety energy conversion engineering conference; 1974.

8. Skyllas-Kazacos M, Rychick M, Robins R. All-Vanadium Redox Battery 1988.

9. Tokuda N, Kumamoto T, Shigematsu T, Deguchi H, Ito T, Yoshikawa N, Hara T. Development of a redox flow battery system. sumitomo electric technical review - English edition- 1998:88-94.

10. Skyllas-Kazacos M, Kazacos M, McDermott R. Vanadium compound dissolution processes. Patent Application PCT/AU1988/000471 1988.

11. Zhao Y. Advanced charged sponge-like membrane with ultrahigh stability and selectivity for vanadium flow batteries. 2016.

12. Ya-Ching Tseng. Design, construction, and study of performance improvement in a vanadium redox flow battery. The Pennsylvania State University; 2011.

13. Nguyen T, Savinell RF. Flow batteries. Interface 2010, 54-56.

14. B. Huskinson, M.P. Marshak, C. Suh, S. Er, M.R. Gerhardt, C.J. Galvin, X. Chen, A. Aspuru-Guzik, R.G. Gordon and M.J. Aziz. A metal-free organic-inorganic aqueous flow battery. Nature 2014;505(195).

15. Janoschka T. An aqueous, polymer-based redox-flow battery using non-corrosive, safe, and low-cost materials. 2015.

16. Wang W. Redox flow batteries go organic. 2016.

17. Tayal DC. Electricity and magnetism. Mumbai, IND: Himalaya publishing house; 2009. ID: 10415192.

18. Ngamsai K, Arpornwichanop A. Study on mechanism and kinetic of air oxidation of V (II) in electrolyte reservoir of a vanadium redox flow battery. Energy Procedia 2014;61:1642-5.

19. Zhijiang Tang. Characterization techniques and electrolyte separator performance investigation for all vanadium redox flow battery. University of Tennessee - Knoxville; 2013.

20. Powerwall Tesla home battery [Internet] [cited 2016 03/29]. Available from: https://www.teslamotors.com/powerwall?redirect=no.

21. Advanced Membranes for VRFB. A Collaboration with SNL, PNNL and ORNL [Internet]; c2012 [cited 2016 03/29]. Available from: http://www.sandia.gov/ess/docs/pr_conferences/2012/papers/Friday/Session2/01_Fujimoto_PeerReview_Presentation_2012.pdf.

22. AvCarb P75 [Internet]; c2016 [cited 2016 03/29]. Available from: http://fuelcellstore.com/fuel-cell-components/gas-diffusion-layers/carbon-paper/avcarb-p75.

23. High Purity Vanadium compound [Internet]; c2016 [cited 2016 03/29]. Available from: http://www.alibaba.com/product-detail/bottom-price-high-purity-vanadium-pentoxide_965485441.html?spm=a2700.7724857.29.19.T3U5gU&s=p.

24. 98% H2SO4 Industrial Sulfuric Acid [Internet]; c2016 [cited 2016 03/29]. Available from: http://www.alibaba.com/product-detail/98-H2SO4-Industrial-Sulfuric-Acid-Price_60168573426.html?spm=a2700.7724857.29.79.Gi1A7R.

25. Rychcik M, Skyllas-Kazacos M. Characteristics of a new all-vanadium redox flow battery. J Power Sources 1988 1 January 1988;22(1):59-67.

26. Kazacos M, Kazacos MS. High energy density vanadium electrolyte solutions, methods of preparation thereof and all-vanadium redox cells and batteries containing high energy vanadium electrolyte solutions 2006.

27. Skyllas-Kazacos M, Kazacos M. State of charge monitoring methods for vanadium redox flow battery control. J Power Sources 2011;196(20):8822-7.

28. Brooker RP, Bell CJ, Bonville LJ, Kunz HR, Fenton JM. Determining vanadium concentrations using the UV-Vis response method. Journal of the Electrochemical Society 2015 January 01;162(4):A608-13.

29. Apple Rubber Products. Seal design guide. Available from: http://www.applerubber.com/

30. Vanadium Redox (VRB) Flow Batteries [Internet]; c2016 [cited 2016 03/29]. Available from: http://energystorage.org/energy-storage/technologies/vanadium-redox-vrb-flow-batteries.